

1 Ideas and perspectives: Mineralizing Fluid Control  
2 on ~~Minor~~Foreign Elements in Biogenic CaCO<sub>3</sub>:  
3 Insights from Otoliths

4 Athina Kekelou\*<sup>1</sup>, Gerald Langer\*<sup>1, 42</sup>, Patrizia Ziveri<sup>1, 2, 3, 4</sup>

5 <sup>1</sup> Institute of Environmental Science and Technology (ICTA-UAB), Universitat Autònoma de Barcelona,  
6 08193, Bellaterra, Spain

7 <sup>2</sup> [Marine Biogeosciences, Alfred Wegener Institute, Helmholtz-Zentrum für Polar- und Meeresforschung,](#)  
8 [27570 Bremerhaven, Germany](#)

9 <sup>3,3</sup> Catalan Institution for Research and Advanced Studies, ICREA, 08010, Barcelona, Spain

10 <sup>3,4</sup> Departament de Biologia Animal, de Biologia Vegetal i d'Ecologia, Universitat Autònoma de Barcelona,  
11 Bellaterra, Spain

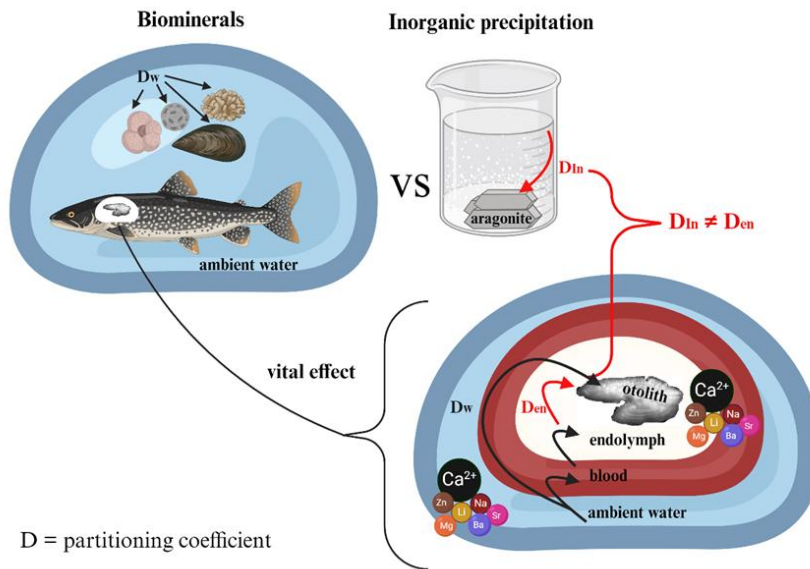
12 \*These two authors contributed equally to this work.

13 ~~Corresponding~~ Correspondence to: [Athina.Kekelou@uab.cat](mailto:Athina.Kekelou@uab.cat) & [Gerald.Langer@uab.cat](mailto:Gerald.Langer@uab.cat) ~~aw.de~~

14 Keywords

15 Endolymph, otolith, partitioning of minorforeign elements, biomineralization, vital effect

16 Graphical Abstract



17

18 **Key Figure (Graphical Abstract)** “Mineralizing Fluid Control on MinorForeign Elements in Biogenic CaCO<sub>3</sub>:

19 Insights from Otoliths” Created in BioRender. Kekelou, A. (2024) BioRender.com/s39g673

20 Abstract

21 The minorforeign element composition of calcium carbonate (CaCO<sub>3</sub>) biominerals from marine calcifying  
22 organisms leaving a sedimentary record has been used for decades to reconstruct various biogeochemical  
23 parameters. Advancing geochemical proxies and understanding their underlying mechanisms is essential  
24 for climate reconstructions, environmental research, and investigations of biomineralization processes.  
25 Despite considerable success of proxy applications, limited mechanistic understanding still restricts their  
26 full potential. The problem is often summarized by the term “vital effect”, i.e. minorforeign element  
27 partitioning due to biological activity. The element partitioning from the calcifying fluid into the biomineral,  
28 however, is usually described in terms of inorganic precipitation of a mineral from an aqueous solution of  
29 inorganic ions. Although this assumption is central to many partitioning models it has not been tested

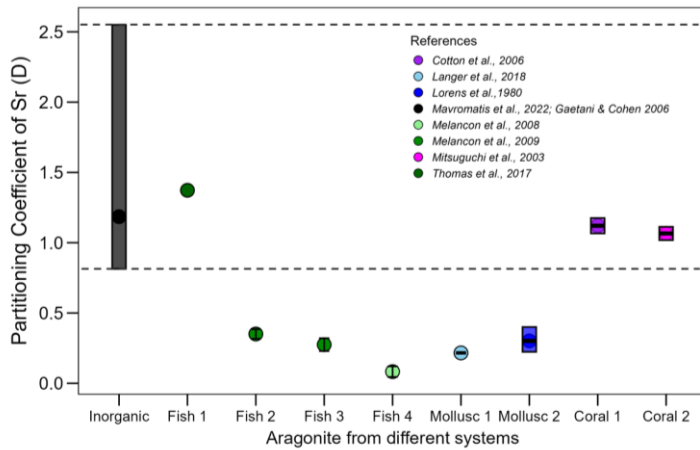
30 because the calcifying fluid of classic proxy archives such as foraminifera, molluscs, and coccolithophores  
31 has not been successfully sampled for element analysis. The calcifying fluid of fish otolith formation  
32 (endolymph), by contrast, was sampled and chemically analysed accompanied by corresponding otolith  
33 data. However, previous datasets have not been compared to inorganic partitioning coefficients to test this  
34 assumption. In this study, we address this gap using published data from four fish species and six elements.  
35 Our results indicate that the final stage of otolith [minorforeign](#) element incorporation is influenced by  
36 organic matter in the endolymph fluid and therefore cannot be considered purely inorganic. Our conclusion  
37 questions a central assumption of many [minorforeign](#) element partitioning models. This does not imply that  
38 existing models are questionable, but that they share a common oversimplification. By removing this  
39 oversimplification all kinds of different models can be improved. Our study contributes broadly to the  
40 understanding of biogenic CaCO<sub>3</sub> geochemistry, and it is relevant to the majority of existing models.

## 41 1. Introduction

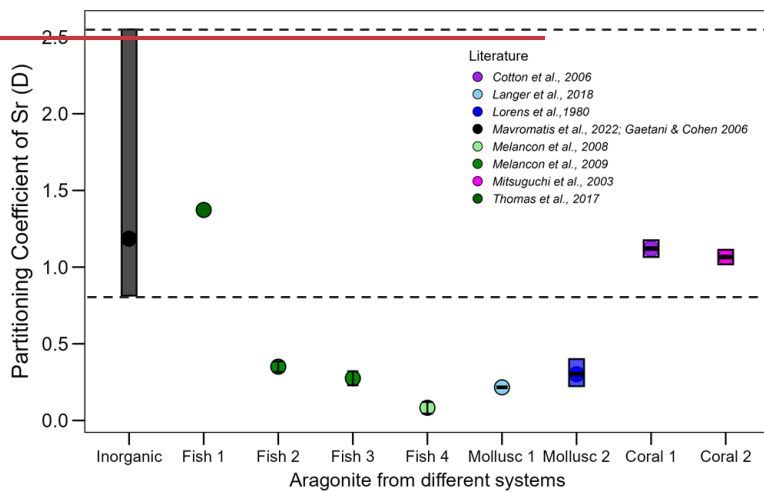
42 The [minorforeign](#) element (Me) and isotopic composition of marine calcium carbonate (CaCO<sub>3</sub>) (mostly  
43 aragonite and calcite) biominerals from the sedimentary record has been used as a proxy for the  
44 reconstruction of specific environmental parameters such as seawater temperature since the 1950s (Katz et  
45 al., 2010; Urey et al., 1951). These geochemical proxies are instrumental in e.g. detecting effects of  
46 anthropogenic climate change on marine calcifying organisms (calcifiers) ([Druffel E.R.M. 1997.; Katz et](#)  
47 [al., 2010](#); Pallacks et al., 2023). A geochemical paleo-proxy application requires a correlation of the proxy  
48 with the target environmental parameter, and this is traditionally achieved by various calibration methods  
49 (Allen et al., 2016; Elderfield & Ganssen, 2000). The calibration of a geochemical proxy alone, however,  
50 does convey little knowledge about the processes underlying proxy signals and accuracy. This knowledge  
51 is, however, essential for developing a mechanistic understanding of the proxy and eventually will enable  
52 us to predict proxy signals using conceptual biomineralization models (Nehrke & Langer, 2023).  
53 Biomineralization models, as opposed to calculations premised on precipitation of the mineral from  
54 seawater, are required because marine calcifiers used as proxy archives do not precipitate their hard parts  
55 from seawater but from a special calcification fluid thereby introducing the problem of the vital effect  
56 (Nehrke & Langer, 2023; Urey et al., 1951). This calcification fluid is localised in the so-called site of  
57 calcification (SOC). Different proxy-archive forming calcifiers have SOC's formed by different structures  
58 such as pseudopodia (foraminifera, single-celled calcifying organisms), mantle epithelium (molluscs,

59 invertebrate animals that form a calcified shell), or intracellular vesicles (coccolithophores, single-celled  
60 calcifying algae) (Angell, 1967; Crenshaw, 1972; Langer et al 2021, Wilbur & Watabe, 1963).

61 In all cases, however, the proxy signal will be influenced by the transport of ions from seawater into the  
62 SOC (Nehrke & Langer, 2023). This transport can introduce partitioning steps that render the overall  
63 partitioning different from what would be expected based on inorganic precipitation from seawater. A  
64 striking example is the Sr/Ca signature in diverse calcifiers (Fig. 1). The data selected for Fig. 1 from the  
65 aragonite literature illustrate that the Sr partitioning coefficient ( $D_{Sr} = (Sr/Ca)_{\text{biomineral}} / (Sr/Ca)_{\text{seawater}}$ ) in  
66 some cases falls within the range of inorganic precipitation, in others it does not. We selected Sr  
67 incorporation in aragonitic biominerals here, but a well-known riddle is the Mg-problem, as it is often  
68 informally referred to, in calcitic biominerals. Specifically, the fact that Mg/Ca does not simply reflect  
69 inorganic temperature-modulated partitioning but is strongly affected by biological (vital) effects.  
70 Organisms can actively regulate Mg transport, potentially resulting in calcifying fluids with varying Mg/Ca  
71 ratios. Additionally, Mg might partly reside in the organics of a biomineral (Schöne et al 2010), as opposed  
72 to the mineral phase (Branson et al 2013) exhibiting different partitioning behaviour in organic and mineral  
73 phase respectively. These factors might cause biomineral Mg/Ca to deviate from what would be expected  
74 from inorganic precipitation from seawater (Bentov & Erez, 2006; Nehrke et al., 2013).”but a well-known  
75 riddle is the Mg-problem, as it is often informally referred to, in calcitic (Bentov & Erez, 2006; Nehrke et  
76 al., 2013)



77



78

79 **Figure 1.** Sr partitioning coefficient range ( $DSr = (Sr/Ca)_{\text{biomineral}} / (Sr/Ca)_{\text{seawater}}$ ) observed in different  
 80 organisms with aragonite biominerals (shown in various colors) compared with the range for inorganic aragonite (black  
 81 bar, with the full range indicated by the dashed black line). The references of the data are listed in the figure legend.  
 82 Sr partitioning coefficient range ( $D_{Sr} = (Sr/Ca)_{\text{biomineral}} / (Sr/Ca)_{\text{seawater}}$ ) in different organisms with aragonite biominerals  
 83 (different colours) and the inorganic aragonite the black bar (range highlighted with dashed black line). The literature  
 84 of the data is given in the caption of the figure.

85 -An intuitive, and often used, assumption is that knowledge of the ionic composition of the calcifying fluid  
 86 would solve this problem. In other words, it is expected that a partitioning coefficient calculated using the  
 87 calcifying fluid minor/foreign element (Me) to Ca ratio (Me/Ca) will fall within the range of values

88 determined in inorganic precipitation experiments (Elderfield et al., 1996; Langer et al., 2006, 2016, 2018;  
89 Stoll et al., 2012). Unfortunately, the SOCs of most classic proxy-archive forming calcifiers are too small  
90 to be sampled for element analysis (Checa, 2018; Kadan et al., 2021; Nomaki et al., 2018). Therefore,  
91 various model approaches have been developed to calculate ~~minor~~foreign element partitioning into  
92 biominerals (D’Olivo & McCulloch, 2017; Elderfield et al., 1996; Hohn & Merico, 2015; Langer et al.,  
93 2006, 2016; Nehrke & Langer, 2023; Ziveri et al., 2003, 2012). These models have provided new insights  
94 into the relationship between conceptual biomineralization models and ~~minor~~foreign element partitioning,  
95 but they have, yet, failed to predict partitioning patterns based solely on independent constraints (Nehrke  
96 & Langer, 2023). Therefore, these models rely on assumptions, many of which do not account for the  
97 complexity of ~~minor~~foreign element partitioning during biomineral formation. It is, for example, by no  
98 means self-evident that a partitioning coefficient calculated using the calcifying fluid composition will fall  
99 within the range of inorganic values.

100 Table 1. Summary of commonly studied geochemical elements in fish otoliths, their targeted environmental or  
101 biological variables, proxy types, specific elemental ratio, relevant ecosystems, and key references.

Targeted Variable	Proxy Type	Specific elemental ratio	Ecosystem	References
Temperature	Elemental Ratios, Stable Isotope	Sr/Ca, Mg/Ca, Li/Ca, Mn/Ca, Ba/Ca, Cu/Ca, $\delta^{18}\text{O}$	Marine & Estuarine	(Cavole et al., 2023; Devereux, 1967; Miller & Hurst, 2020; Mondal et al., 2022; Morat et al., 2023; Rosales et al., 2004; Tanner et al., 2013; Willmes et al., 2019)
Salinity	Elemental Ratios, Stable Isotope	Sr/Ca, Ba/Ca, Mn/Ca, $\delta^{18}\text{O}$ , $^{87}\text{Sr}/^{86}\text{Sr}$	Estuarine & Freshwater	(Höpker et al., 2022; Kerr et al., 2007; Nelson & Powers, 2020; Rosales et al., 2004)
Oxygen, Hypoxia	Elemental Ratio	Mn/Ca, Mg/Mn	Marine	(Limburg et al., 2011, 2015; Limburg & Casini, 2018)
Diet, Metabolism, Physiology	Elemental Ratios, Stable Isotope	$\delta^{13}\text{C}$ , $\delta^{15}\text{N}$ , Li/Ca, Mg/Ca	Marine	(Chung et al., 2019; Izzo et al., 2018; Lall & Kaushik, 2021; J. Lueders-Dumont, 2024; J. A. Lueders-Dumont et al., 2018; Martino et al., 2020, 2021; Rao et al., 2024; Shiao et al., 2018; Sirot et al., 2017; A. Sturrock et al., 2014)
Ontogeny, Life History	Elemental Ratios, Stable Isotope	Sr/Ca, Ba/Ca, Mg/Ca, $^{87}\text{Sr}/^{86}\text{Sr}$	Marine & Freshwater	(Campana, 1999; Campana & Thorrold, 2001; Halden & Friedrich, 2008; Kennedy et al., 2002; Longmore et al., 2011; Saygin et al., 2022; Wells et al., 2014; Zazzo et al., 2006)
Migration, Habitat	Elemental Ratios, Stable Isotope	Sr/Ca, Ba/Ca, Mn/Ca, $\delta^{18}\text{O}$ , $\delta^{13}\text{C}$	Marine & Freshwater	(Avigliano et al., 2015; Fraile et al., 2016; Phillis et al., 2011; Sackett et al., 2024;

Stock Discrimination	Elemental Ratios, Stable Isotope	Sr/Ca, Ba/Ca, Mg/Ca, <sup>87</sup> Sr/ <sup>86</sup> Sr	Marine	Sturrock et al., 2012; Walther & Limburg, 2012) (Campana & Thorrold, 2001; Longmore et al., 2011; Padilla et al., 2015; Vaisvil et al., 2023)
----------------------	-------------------------------------	---	--------	--

102

103 In this paper, we focus on fish otoliths, mostly aragonitic biominerals in the inner ears of bony fish, that are  
 104 an understudied and underappreciated model system to address element partitioning patterns (Hüssy et al.,  
 105 2020; Melancon et al., 2005). Otoliths can be found as fish remains in the sedimentary record (Elder et al.,  
 106 1996; Mellars et al., 1980) and they have been used in many ways in fisheries research, ecology, and the  
 107 reconstruction of fish stock environments (Reis-Santos et al., 2023). The ~~minor~~foreign element  
 108 compositions of otoliths can serve as proxies for e.g. migration patterns, salinity, and temperature  
 109 (Albertsen et al., 2021; Bath Martin & Thorrold, 2005; Shiao et al., 2006). The otolith isotopic composition  
 110 is also used as a proxy, e.g. habitat/migration is inferred from Sr and C isotopes, and dietary history from  
 111 N and C isotopes, while O isotopes provide information about temperature and salinity (see Table 1 for an  
 112 overview of otolith-based geochemical proxies). Otoliths serve as valuable proxy archives for several  
 113 reasons: a) Unlike coccolithophores (which have coccoliths ranging from 2 to 20 µm) and require complex  
 114 species-specific separation, otoliths allow monospecific analyses; b) ~~Unlike planktonic foraminifera that~~  
 115 ~~live and calcify mainly in exclusively in marine environments and benthic foraminifera that are found also~~  
 116 ~~in brackish environments, whereas fish otoliths biomineralize in teleost fishes across marine, brackish, and~~  
 117 ~~freshwater habitats, providing a potential archive of environmental conditions across diverse that spans~~  
 118 ~~diverse aquatic systems;” Unlike foraminifera, otoliths are found in marine, freshwater, and estuarine~~  
 119 ~~environments, making them broadly applicable across aquatic systems;~~  
 120 c) Element-to-calcium ratios in individual otoliths can be spatially mapped, offering insights into the fish  
 121 life history traits and seasonal patterns.

122 As with any other proxy archive, otolith-based proxies are subject to secondary influences. For example,  
 123 Sr/Ca and Ba/Ca are influenced by their correspondent concentrations in ambient water, but also salinity  
 124 and temperature (Hüssy et al., 2021).

125 It has also been noted that, besides environmental parameters, physiology influences ~~minor~~foreign element  
 126 and isotope composition (Bareille et al., 2024; Izzo et al., 2018; Sturrock et al., 2015). The value of otoliths  
 127 as geochemical proxy archives has been highlighted but is also, unsurprisingly, critically discussed (Hüssy  
 128 et al., 2021; Thomas & Swearer, 2019; Walther, 2019). The latter authors emphasize that future steps

129 towards improving otolith proxy applications critically include an understanding of the processes bringing  
130 about the proxy signal. Hüssy et al., (2021) effectively summarize the fundamental processes governing  
131 elemental and isotope fractionation into otoliths. They distinguish ion transport into the endolymph from  
132 “biomineralization” by which they mean the formation of the otolith within the endolymph. Note that often  
133 the term “biomineralization” covers both ion transport and formation of the biomineral within the SOC  
134 (Nehrke and Langer 2023). As for foraminifera, there has been an increasing interest in the relationship  
135 between partitioning (usually called fractionation when referring to isotopes) patterns and biomineralization  
136 concepts in otoliths (Campana, 1999; Hüssy et al., 2021). To understand even the most straightforward and  
137 useful proxies, such as Sr/Ca in foraminifera, both biological and inorganic processes need to be considered  
138 (Langer et al 2016). Otoliths offer the unique opportunity to study the fractionation processes within the  
139 SOC in greater detail than is possible in classic proxy archives such as foraminifera.

140 An outstanding feature of otolith formation is the fact that the calcifying fluid, i.e. the endolymph, has such  
141 a large volume that it can be sampled for element analysis (Kalish, 1989). This offers the unique opportunity  
142 to measure minor/foreign element composition of both the biomineral and its parent solution (Allemand et  
143 al., 2007; Edeyer et al., 2000; Kalish 1989, 1991; Melancon et al., 2005, 2008, 2009a; Payan et al., 1997,  
144 1998, 1999, 2002, 2004; Thomas et al., 2017). Although some of the latter studies provide the relevant data  
145 and discuss the relationship between partitioning and biomineralization processes, no study has addressed  
146 the following question: is the minor/foreign element partitioning coefficient from endolymph into otolith  
147 (in the following called  $D_e$ ) numerically equivalent to the one from an aqueous solution of inorganic ions  
148 into aragonite? Here we therefore use the relevant datasets in the literature to address this question. We look  
149 at six different minor/foreign elements in four different species, one marine and three freshwater ones. We  
150 compare minor/foreign element partitioning coefficient from endolymph to otolith with partitioning  
151 coefficient from inorganic aragonite precipitation. This study provides a deeper mechanistic understanding  
152 of the vital effect by identifying one, so far neglected, locus of the vital effect in the calcifying organism.  
153 The aim is to test the commonly made assumption that biogenic partitioning coefficients should be  
154 indistinguishable from inorganic ones if the Me/Ca of the actual parent solution (the calcifying fluid) of  
155 biomineral formation is used as denominator (e.g. Langer et al., 2006). Our results suggest that partitioning  
156 of minor/foreign elements from endolymph into otolith cannot be modelled solely in terms of aragonite  
157 precipitation from an aqueous solution of inorganic ions. Our conclusion not only has implications for proxy

158 understanding but also for biomineralization concepts because the latter centrally feature ideas about the  
159 composition of the calcifying fluid and its effect on biomineral formation.

160 2. Material and methods

161 2.1 Data collection and data handling

162 Literature data on Me/Ca ratios in endolymph and otolith were used to calculate partitioning coefficient.

163 The latter were compared to partitioning coefficient determined in inorganic precipitation experiments. The

164 literature data used are summarized in Table 2.

165 Table 2. Literature data used in this study.

System/Organism	Elements	Reference
Inorganic aragonite	Ba	{Gaetani & Cohen, 2006; Mavromatis et al., 2018; Dietzel et al., 2004}
Inorganic aragonite	Mg	{Gaetani & Cohen, 2006; Mavromatis et al., 2022}
Inorganic aragonite	Sr	{Brazier et al., 2023; Gaetani & Cohen, 2006; Zhong & Mucci, 1989; Dietzel et al., 2004}
Inorganic aragonite	Li	{Marriott et al., 2004; Brazier et al., 2024b}
Inorganic aragonite	Zn	{Brazier, et al., 2024a}
Inorganic aragonite	Na	{Kawabata et al., 2021; Brazier et al., 2024b}
<i>Acanthopagrus butcheri</i> (Fish_S1)	Mg, Sr, Ba, Li	{Thomas et al., 2017}
<i>Lota lota</i> (Fish_S2)	Mg, Sr, Ba, Zn, Na	{Melancon et al., 2009}
<i>Salvelinus namaycush</i> (Fish_S3)	Mg, Sr, Ba, Zn, Na	{Melancon et al., 2009}
<i>Sander vitreus</i> (Fish_S4)	Mg, Sr, Ba, Zn, Na	{Melancon et al., 2008}
<i>Patella caerulea</i> (mollusc1)	Sr	{Langer et al., 2018}
<i>Mytilus edulis</i> (mollusc2)	Sr	{Lorenz & Bender, 1980}
<i>Lophelia pertusa</i> (coral1)	Sr	{Cohen et al., 2006}
<i>Porites australiensis</i> (coral2)	Sr	{Mitsuguchi et al., 2003}
Sea Water	Sr	{Broecker, W. S., & Peng, T.-H. 1982}

Formatted Table

166

167 The literature on inorganic system provides many measurements of the partitioning coefficient ( $D_{in}$ ) from

168 different experimental designs. We selected the full range of values to get a realistic overall picture of the

169 inorganic system. For the otolith-endolymph system the literature was limited. Only three papers gave us

170 enough data to estimate the partitioning coefficient of the elements into the otolith. ~~In the~~The first study

171 ~~of~~by Thomas et al., 2017 they used a marine species, *Acanthopagrus butcheri* (Sp1), and the number of

172 individuals measured was  $N = 3$ . Otoliths were diluted and measured ~~with an in~~ inductively coupled plasma

173 ~~mass spectrometer (ICP-MS)~~the same ~~plasma~~ mass spectrometry (ICP-MS) as the endolymph fluid. They

174 provide the concentration of ~~minor/foreign~~ elements ( $[Me]$ - $[Me]$ ) normalized to the concentration calcium

175 of ( $[Ca]$   ~~$[Ca]$~~ ) in the otolith and the endolymph ratio,  $R = [Me](mmol)/[Ca](mol)$  with the  $\pm sd$  and the

176  $range(R) = \min(R) - \max(R)$ , as well the partitioning coefficient ( $D \times 100$ ). We estimate the range of

177 the  $D$  using a simple formula of range ratio (Eq. 1):

178 
$$range(D_e) = \max(D_e) - \min(D_e) = \left( \frac{\max(R_{otolith})}{\min(R_{endolymph})} \right) - \left( \frac{\min(R_{otolith})}{\max(R_{endolymph})} \right) \quad (1)$$

179 ~~The second and third~~In the other two available paper studies with data meeting the criteria required ~~to for~~  
 180 ~~these estimates, provide data~~were in a form of “the concentration of ~~minorforeign~~ elements” in the otolith  
 181 and in the endolymph (Melancon et al., 2008, 2009a). The species that were used in these studies were the  
 182 freshwater species burbot *Lota lota* (Sp2), lake trout *Salvelinus namaycush* (Sp3) and a walleye *Sander*  
 183 *vitreus* (Sp4), the number of the individuals (N) that were used were  $N_{\text{burbot}}=18$  and  $N_{\text{trout}}=11$  and  $N_{\text{walleye}}=8$ ,  
 184 respectively. In these studies, the concentrations of the elements in the otoliths were quantified by laser  
 185 ablation (LA-ICP-MS) and they performed a series of ablations at the growing otolith edges that were in  
 186 contact with the endolymph and represent the last 30 to 60 days of growth. They provide the average  
 187 concentration of the ~~minorforeign~~ elements  $av[Me] \pm sd$  (ppm) in the otolith and in the endolymph,  
 188 which we converted to mmol/mol. The ratio  $R = [Me](mmol)/[Ca](mol)$  in the otolith and in the  
 189 endolymph and the  $av(D) \pm sd(D)$  was estimated using Eq. (2) and (3)

$$190 \quad av(D_e) = \frac{av(R_{\text{otolith}})}{av(R_{\text{endolymph}})} \quad (2)$$

$$191 \quad sd(D_e) = av(D_e) \times \left( \sqrt{\left( \frac{sd(R_{\text{otolith}})}{av(R_{\text{otolith}})} \right)^2} + \sqrt{\left( \frac{sd(R_{\text{endolymph}})}{av(R_{\text{endolymph}})} \right)^2} \right) \quad (3)$$

Formatted: No bullets or numbering

## 192 2.2 Partitioning coefficient estimations

Formatted: Font: 11 pt, Font color: Auto, English (United States)

193 Then the ratio and the partitioning coefficient, in the different parts of the ion transport pathway that the  
 194 elements need to cross to precipitate in the otolith, were estimated. Only one paper provided sufficient data  
 195 for this purpose (Melancon et al., 2009). The ion transport pathway starts from the ambient water to blood,  
 196 then from blood to endolymph and the final step is from endolymph to otolith (Graphical Abstract). The  
 197 partitioning coefficient that describes the last step of endolymph to otolith was estimated ~~using the equation~~  
 198 ~~4(Eq. 4)~~. Some extra variables were also estimated. The first was the D commonly used in biomineralization  
 199 studies. This  $D_w$  is the partitioning coefficient using as parent solution the ambient water (Eq. 5). The other  
 200 two Me/Ca were estimated based on the idea that the last step of the precipitation is purely inorganic (Eq.  
 201 7) and (Eq. 8). The first of those (Eq. 7), is the ratio that the otolith would have, if the last precipitation step  
 202 was completely inorganic and the parent solution was the endolymph ( $R_{\text{otolith1}}$ ). The second (Eq. 8) is the  
 203 theoretical ratio if the parent solution was water ( $R_{\text{otolith2}}$ ).

204 
$$D_e = \frac{R_{otolith}}{R_{endolymph}} \quad (4)$$

205 
$$D_w = \frac{R_{otolith}}{R_{water}} \quad (5)$$

206 
$$D_{In} = \frac{R_{crystal}}{R_{fluid}} \quad (6)$$

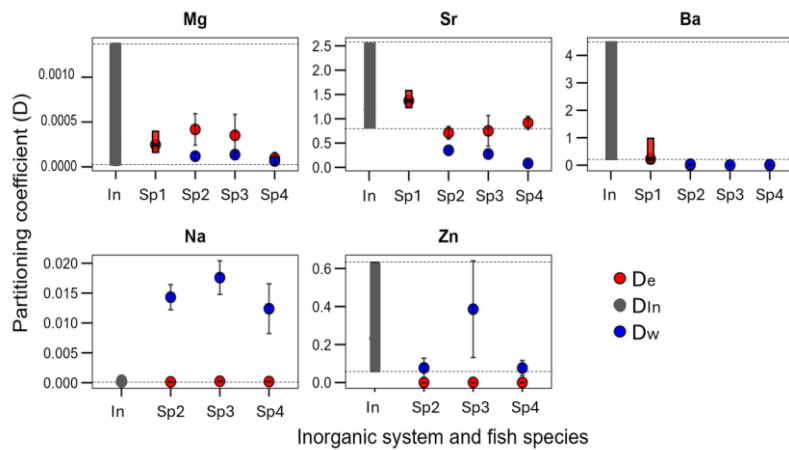
207 
$$R_{otolith1} = range(D_{In}) \times R_{endolymph} \quad (7)$$

208 
$$R_{otolith2} = range(D_{In}) \times R_{water} \quad (8)$$

209 We address the following question. Does the numerical value of the minor/foreign element partitioning  
210 coefficient from endolymph into otolith equal that of the partitioning coefficient from an aqueous solution  
211 into pure aragonite? As mentioned in the introduction, Fig. 1 illustrates the range of the Sr partitioning  
212 coefficient (D) in different calcifying marine organisms, we used as parent solution seawater and the ratios  
213 of the elements in each organism from the literature (Broecker & Peng, 1982; Cohen et al., 2006; Langer  
214 et al., 2018; Lorens & Bender, 1980; Mitsuguchi et al., 1996).

### 215 3. Results

216 The partitioning coefficient of various foreign elements from four fish species was comparatively analyzed  
217 with the inorganic partitioning coefficient of the same element (Fig. 2). To elaborate further, the distinct  
218 environments have a different impact on Ba, which exhibit divergent patterns among marine and freshwater  
219 species. We observe that for Ba in the Sp1 (marine) their D is within the range of inorganic values while  
220 the Sp2, Sp3, Sp4 are below the inorganic range. This phenomenon stands in contrast to the behavior  
221 observed in Mg that all fish otoliths D are in the range of the inorganic  $D_{In}$  of Mg. The  $D_e$  of the elements  
222 Na and Sr, with the borderline case of Sr in one fish (Sp2), fall within the inorganic range when the  $D_w$  does  
223 not. Zn represents a distinctive case; while  $D_w$  appears to be within the range of the inorganic system,  $D_e$  is  
224 not. A comprehensive analysis of the available evidence suggests that the "vital effect" manifests in some  
225 elements while remaining invisible in others. The supplementary material contains the partitioning  
226 coefficient  $D_e$  of Li in only for the Sp1 which is above the  $D_{In}$  of Li.



227

228 **Figure 2** The partitioning coefficient (D) per element (Mg, Sr, Ba, Na, Zn), the range of the inorganic system (In) and

229 the mean±SD of the D in three different freshwater fish burbot *Lota lota* (Sp2), lake trout *Salvelinus namaycush* (Sp3)

230 and a walleye *Sander vitreus* (Sp4) and the range of the marine fish the *Acanthopagrus butcheri* (Sp1). Colour code:

231 red is the D<sub>e</sub> (endolymph as parent solution) and blue the D<sub>w</sub> (water as parent solution) for fish and black is the D<sub>In</sub>

232 of the inorganic aragonite.

233 The ion transport pathways of five distinct elements of the Sp2 otolith are demonstrated (Fig. 3) and for the

234 Sp3 (Fig. S2). The ratios of elements normalized to calcium (Ca) were measured in different solutions to

235 trace their transport pathway into the otolith. Foreign elements of the ambient water pass to the blood and

236 then to the endolymph where the biomineral is precipitated. The largest partitioning steps occur during the

237 transition from water to blood and from endolymph to otolith. Despite the different patterns in the outcomes,

238 it has been demonstrated that, in certain instances, the occurrence of the vital effect is visible as evidenced

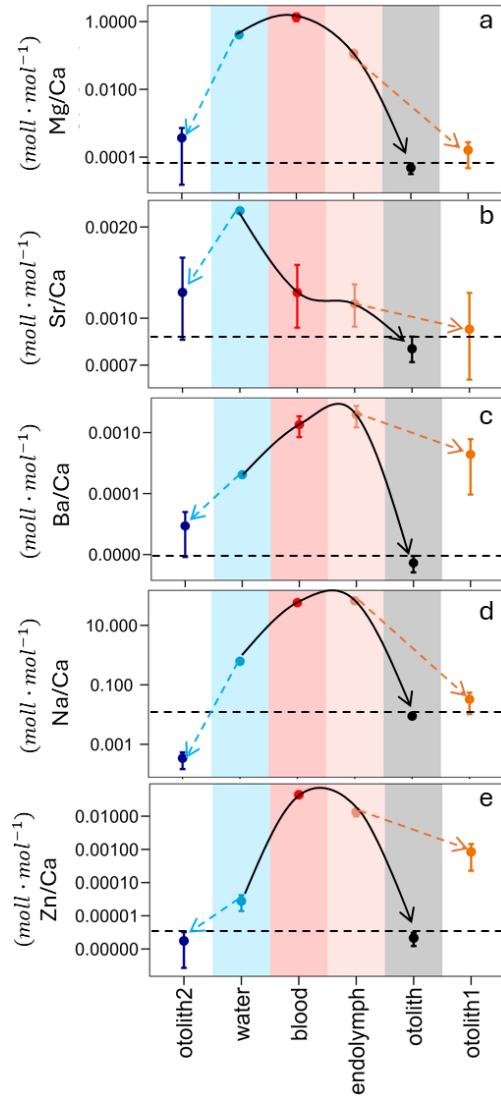
239 by the observation of a discrepancy in otolith1 relative to otolith (Fig. 3, c, e). Conversely, in other instances,

240 the vital effect remains invisible, (Fig. 3, a, b, d).

Formatted: Font: 9 pt

Formatted: Font: 9 pt

Formatted: Font: 9 pt

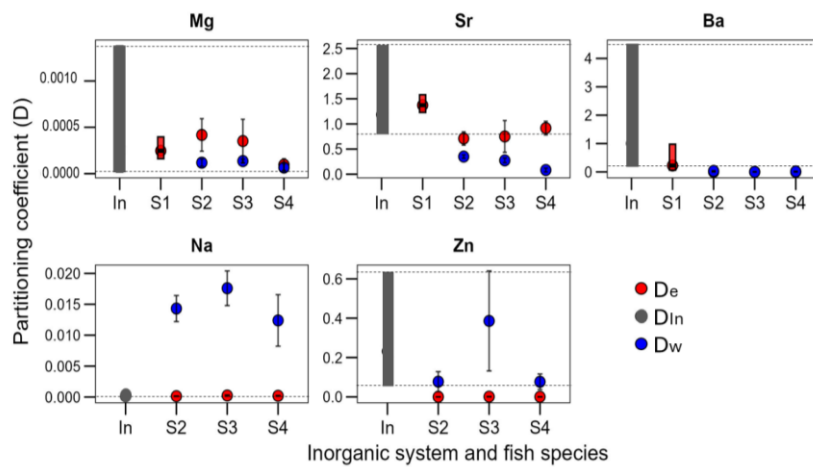


241

242 **Figure 3** Me/Ca of burbot *Lota lota* (Sp2) in different reservoirs indicated by colored areas. The white areas (otolith 1  
 243 and otolith 2) do not represent measured values but are calculated according to  $otolith1 = D_{In} * (Me/Ca)_{endo}$ , and  
 244  $otolith2 = D_{In} * (Me/Ca)_{water}$ . For  $D_{In}$  we used either the minimum or the maximum value depending on which one  
 245 would minimize the offset between (Me/Ca) otolith-measured and (Me/Ca) otolith-calculated. The error bar represents  
 246 the range of the values that the system can reach. a) is the pathway of Mg, b) the pathway of Sr, c) the pathway of Ba,  
 247 d) the pathway of Na and e) the pathway of Zn. All the data are displayed on a log<sub>10</sub>-scaled y-axis.

248 **1. Results**

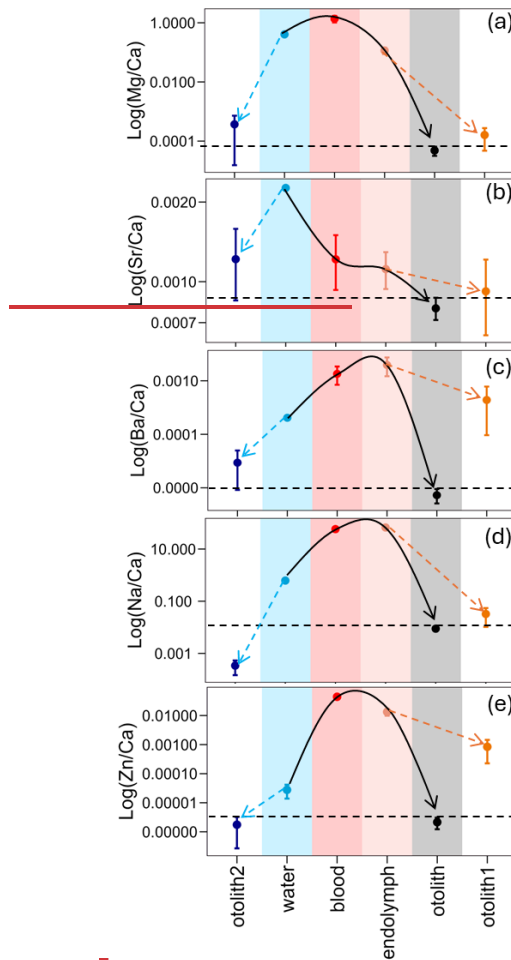
249 Figure 2 illustrates the partitioning coefficient of different minor elements from different fish species were  
 250 compared numerically with the inorganic partitioning coefficient of the same element. To elaborate more  
 251 the distinct environments, affect Ba and Sr, which demonstrate different behaviour for the marine and  
 252 freshwater species something that is not observed in the other elements. For the freshwater fish were  
 253 estimated both partitioning coefficient from water ( $D_w$ ) and from endolymph ( $D_e$ ) because data were  
 254 available. The  $D_e$  of the elements Na and Sr, except for one fish (S2), fall within the inorganic range when  
 255 the  $D_w$  does not. Additionally, Ba and Mg in both  $D_e$  and  $D_w$  yielded comparable results but with difference  
 256 corresponding to the inorganic range. In the case of Ba, the coefficient is not within the inorganic range,  
 257 while in the other instance Mg, it is. Finally, Zn is a unique case because it seems that  $D_w$  is in the range of  
 258 the inorganic system, but  $D_e$  is not. From all this observation we can come to the general result that the  
 259 'vital effect' for some elements is visible and for some invisible. In the supplementary material there is also  
 260 the partitioning coefficient  $D_e$  of Li in the S1 fish.



261 **Figure 2** The partitioning coefficient (D) per element (Mg, Sr, Ba, Na, Zn), the range of the inorganic system (In) and  
 262 the mean  $\pm$  SD of the D in three different freshwater fish burbot *Lota lota* (S2), lake trout *Salvelinus namaycush* (S3)  
 263 and a walleye *Sander vitreus* (S4) and the range of the marine fish the *Acanthopagrus butcheri* (S1). The different colors  
 264 of D values, red is the  $D_e$  (endolymph as parent solution) and blue the  $D_w$  (water as parent solution) for fish and black  
 265 is the  $D_{In}$  of the inorganic aragonite.  
 266

267 Figure 3 illustrates the ion transport pathways of five different elements in the burbot *Lota lota*  
268 otolith. We demonstrate the same idea in Fig. Supp.2 for the *Salvelinus namaycush* (S3). In almost  
269 all cases the ambient water is not sufficient to describe the co-precipitation of Me into otoliths.  
270 The ratios of elements normalized to calcium (Ca) were measured in different solutions to trace  
271 their transport pathway into the otolith. We notice that the precipitation steps from each reservoir  
272 follow the same path with the largest changes in partitioning occur during transfer from water to  
273 blood and from endolymph to otolith. Although we have different outcomes in terms of the final  
274 product the otolith. What we actually see is that knowing that the vital effect is happening in some  
275 cases we observe it, difference in otolith1 with otolith (Fig. 3, (c), (e)) and in some cases it is

276 invisible (Fig.3, (a), (b), (d)). As previously demonstrated in Figure 2, this phenomenon is  
 277 influenced by both elemental and species specific factor.



278  
 279 **Figure 3**  $Me/Ca$  of burbot *Lota lota* (S2) in different reservoirs indicated by colored areas. The white areas (otolith  
 280 1 and otolith 2) do not represent measured values but are calculated according to  $otolith1 = D_{in} * (Me/Ca)_{water}$  and  
 281  $otolith2 = D_{in} * (Me/Ca)_{blood}$ . For  $D_{in}$  we used either the minimum or the maximum value depending on which one  
 282 would minimize the offset between  $(Me/Ca)_{otolith}$  measured and  $(Me/Ca)_{otolith}$  calculated. The error bar represents  
 283 the range of the values that the system can reach. (a) is the pathway of Mg, (b) the pathway of Sr, (c) the pathway of  
 284 Ba, (d) the pathway of Na and (e) the pathway of Zn.

285 3.4.Discussion

286 Here we challenge the assumption that biomineral formation from the calcifying fluid is fully describable  
287 in terms of the formation of synthetic monocrystals from an aqueous solution of inorganic ions. Although  
288 intuitive, this idea might underestimate the complexity of biomineral formation for, inter alia, the following  
289 reasons. Firstly, biominerals are not monocrystals but organo-mineral composite structures, implying the  
290 possibility that minorforeign elements reside in the organic material (Cuif et al., 2010; Hüsey et al., 2021;  
291 Miller et al., 2006; Walker & Langer, 2021) Secondly, the calcifying fluid usually contains organic  
292 molecules, which could interact with inorganic ions thereby decreasing their activity ratios in solution and  
293 hence in the biomineral since mostly free ions are incorporated in the crystal (e.g. Borelli et al., 2001; Hüsey  
294 et al., 2021; Meyer et al., 2020; Moura et al., 2000; Thomas & Swearer, 2019). In the following we show  
295 that both processes do indeed influence minorforeign element distribution into otoliths which is, therefore,  
296 not reducible to inorganic aragonite co-precipitation.

297 4.1 MinorForeign element partitioning from endolymph to otolith cannot be modelled in  
298 terms of inorganic aragonite precipitation

299 We looked at the partitioning coefficient of six elements (Sr, Ba, Mg, Na, Zn, and Li) in four different  
300 species, Sp1-Sp4 (FigFig. 2, Fig Supp-S1). For our question, it is helpful to consider several elements, as  
301 opposed to just one, because results from a single element might be misleading (Langer et al., 2018). A  
302 species comparison will further strengthen the conclusions because the question concerns the endolymph-  
303 otolith system in general. The partitioning coefficients  $D_e$  of Na, Mg (mostly), Sr and Ba (in Sp1) fall within  
304 the range of inorganic values (FigFig. 2, Fig Supp-S-1). For all-othertthe remaining elements, Zn and Li,  
305 otoliths show a partitioning behaviour different from inorganic aragonite. Taken together these results  
306 clearly show that the endolymph-otolith system produces minorforeign element partitioning coefficients  
307 different from the ones determined in synthetic aragonite precipitation. Therefore, we conclude that  
308 minorforeign element partitioning during otolith formation in the endolymph involves processes that do not  
309 occur during inorganic aragonite precipitation. An obvious further question is why the partitioning  
310 behaviour is both element and species specific. In general, the answer will likely involve specific organic  
311 material both in the endolymph and the otolith. In the following we will concretize this somewhat vague  
312 hypothesis.

313 4.2 Element and species specificity of partitioning behaviour

314 Otolith partitioning coefficients  $D_e$  of Ba and Zn (and Sr in Sp2 and partly Sp3) in freshwater species are  
315 lower than those in the inorganic system (Fig. 2). In the case of Sr and Ba incorporation into the organic  
316 part of the otolith seems negligible, ruling out a significant influence of otolith organics on partitioning  
317 (Izzo et al., 2016). This strongly suggests that endolymph organic material (Borelli et al., 2001; Thomas et  
318 al., 2019) forms complexes with divalent cations, fractionating for Sr and Ba. The remaining free ions in  
319 solution are incorporated into the growing otolith aragonite, with minor/foreign element partitioning  
320 depending on crystal growth rate, in turn depending on various factors such as supersaturation,  
321 stoichiometry, and surface topography (Nehrke et al., 2007; Wolthers et al., 2013).

322 An example of organic material fractionating for Sr and Ba are polysaccharides such as alginates (Yuryev  
323 et al., 1979). The situation might be different for Mg which is fractionated against when forming complexes  
324 with organics thereby weakening fractionation against Mg into calcite (Mavromatis et al., 2017; Takeuchi  
325 et al., 2008). Complexation of minor/foreign elements with inorganic ligands can also affect partitioning  
326 into calcium carbonate. In the case of Mg, sulfate complexes lead to an apparently harder fractionation  
327 against Mg into calcite (Goetschl et al., 2019; Mucci et al., 1989). Since for Mg, organic and inorganic  
328 complexes influence partitioning behaviour differently the overall change in the partitioning coefficient  
329 will partly depend on the relative concentrations of these different ligands. Inorganic ligands such as sulfate,  
330 phosphate, and carbonate might play a considerable role in modifying partitioning behaviour in calcifying  
331 fluids. The modification of the partitioning behaviour will be minor/foreign element specific too. While  
332 alkali metal (e.g. Na and Li) complexes are of minor/foreign importance, Zn for example has a high affinity  
333 to form inorganic complexes with e.g. sulfate and carbonate (Krężel & Maret, 2016; Lewis & Randall,  
334 1921; Olsher et al., 1991; Stanley & Byrne, 1990). However, Li partitioning into calcite is pH dependent  
335 (Füger et al., 2019). Since calcifying fluids are likely to feature high pH, Li partitioning into calcitic  
336 biominerals, and maybe aragonitic ones too, might display a “high pH signal”. ~~Additionally, organic  
337 complexes with Zn can comprise the majority of total Zn, for example in surface seawater down  
338 to 500m (Bruland, 1989). These naturally occurring organic ligands in seawater will be important  
339 in calcifiers using seawater as substrate supply for calcification, e.g. foraminifera (Elderfield et  
340 al., 1996). The influence of organic material in the calcifying fluid on minor element partitioning  
341 shows that the localization of the minor element in the mineral part of the biomineral does not~~

342 ~~justify the conclusion that the partitioning process is inorganic. This reasoning has nevertheless~~  
343 ~~been applied to Mg partitioning into foraminiferal calcite (Branson et al., 2013). The latter authors~~  
344 ~~show that Mg resides in foraminiferal calcite and from this observation conclude that the~~  
345 ~~partitioning behaviour of Mg is inorganic. Since Mg is an important temperature proxy (Elderfield~~  
346 ~~& Ganssen, 2000), this example illustrates the usefulness of the endolymph-otolith system for the~~  
347 ~~development of a process-based understanding of proxy signal formation more generally. Please~~  
348 ~~note that foraminiferal shells are calcitic while otoliths are aragonitic. This difference in the~~  
349 ~~calcium carbonate polymorph used by different organisms has implications for numerical values~~  
350 ~~of partitioning coefficients (Langer et al 2018), but has no bearing on the argument made above.~~  
351 ~~We claim that the fact that Mg resides in the mineral phase of a biomineral, as opposed to the~~  
352 ~~organic phase, is not sufficient to support the inference that the partitioning process is a case of~~  
353 ~~inorganic co-precipitation. This claim holds regardless of the calcium carbonate mineral into~~  
354 ~~which Mg is incorporated, and regardless of the Mg/Ca of the respective mineral. Foraminifera~~  
355 ~~for example comprise low Mg (e.g. Ammonia), intermediate Mg (e.g. Amphistegina), and high~~  
356 ~~Mg (e.g. Heterostegina) species (Mewes et al 2014, Mewes et al 2015, Raitzsch et al 2010). In~~  
357 ~~the example mentioned above (Branson et al 2013) both a low Mg species (Orbulina) and an~~  
358 ~~intermediate Mg species (Amphistegina) are discussed. Both the author's argument and our~~  
359 ~~finding are equally applicable to both species, and would be so for any other species.~~

360 Why does Ba partitioning in the marine species Spl differ so strikingly from the one in the freshwater  
361 species (FigFig. 2)? Rather than being a species effect, this might be a methodological effect. Otoliths from  
362 the freshwater species were analyzed by LA-ICP-MS, where only the edge of the otolith was targeted to  
363 achieve a better match with the endolymph analysis (see Material and Methods). Otoliths from the marine  
364 species were dissolved whole for solution analysis by ICP-MS. The Ba/Ca of otoliths can vary substantially  
365 within single otoliths, often with high values near the otolith core (Hermann et al., 2016). This could explain  
366 both the higher De in the marine species and the larger range reaching both below and above the inorganic  
367 range (FigFig. 2).

368 The situation for Zn is different from the one for Sr and Ba because 40-60% of the Zn reside in otolith  
369 organics (McFadden et al., 2016; Miller et al., 2006). Although an effect of endolymph organics cannot be

370 ruled out for Zn, it is equally possible that partitioning into otolith organics is different from partitioning  
371 into otolith aragonite. Differential partitioning between the organic and the mineral part of mollusc shells  
372 has been reported, supporting this possibility (Schöne et al., 2010). Additionally, organic complexes with  
373 Zn can comprise the majority of total Zn, for example in surface seawater down to 500m (Bruland, 1989).  
374 These naturally occurring organic ligands in seawater will be important in calcifiers using seawater as  
375 substrate supply for calcification, e.g. foraminifera (Elderfield et al., 1996). The influence of organic  
376 material in the calcifying fluid on ~~minor~~foreign element partitioning shows that the localization of the  
377 ~~minor~~foreign element in the mineral part of the biomineral does not justify the conclusion that the  
378 partitioning process is inorganic. This reasoning has nevertheless been applied to Mg partitioning into  
379 foraminiferal calcite (Branson et al., 2013). The latter authors show that Mg resides in foraminiferal calcite  
380 and from this observation conclude that ~~the~~its partitioning behaviour of Mg is inorganic. Since Mg is an  
381 important temperature proxy (Elderfield & Ganssen, 2000), this example illustrates the usefulness of the  
382 endolymph-otolith system for the development of a process-based understanding of proxy signal formation  
383 more generally.

384 Please note that foraminiferal shells are calcitic while otoliths are aragonitic. This difference in the calcium  
385 carbonate polymorph used by different organisms has implications for numerical values of partitioning  
386 coefficients (Langer et al 2018), but has no bearing on the argument made above. We claim that the fact  
387 that Mg resides in the mineral phase of a biomineral, as opposed to the organic phase, is not sufficient to  
388 support the inference that the partitioning process is a case of inorganic co-precipitation. This claim holds  
389 regardless of the calcium carbonate mineral into which Mg is incorporated, and regardless of the Mg/Ca of  
390 the respective mineral. Foraminifera, ~~for example~~example example, comprise low-Mg (e.g. *Ammonia*),  
391 intermediate-Mg (e.g. *Amphistegina*), and high-Mg (e.g. *Heterostegina*) species (Mewes et al 2014, Mewes  
392 et al 2015, Raitzsch et al 2010). In the example mentioned above (Branson et al 2013), both a low-Mg  
393 species (*Orbulina*) and an intermediate-Mg species (*Amphistegina*) are discussed. ~~Both~~†The author's  
394 argument, as well as ~~and~~our findings, ~~are~~apply equally applicable to both species; and would ~~be~~do so for  
395 any other species.

396 To sum up, ~~minor~~foreign elements might reside either in the mineral (e.g. aragonite in otoliths) or the  
397 organic part of the biomineral. Partitioning of ~~minor~~foreign elements into the organic part is most likely  
398 different from partitioning into the mineral part. Hence partitioning is not homogeneous across a

399 biomineral. The calcifying fluid often contains organic and, potentially, inorganic ligands that form  
400 complexes with minorforeign elements thereby influencing partitioning into the biomineral.

#### 401 4.3 Biogenic and inorganic partitioning coefficient numerically identical: Mg, Na and Zn

402 The partitioning behaviour of Mg and Na seems to suggest that these elements are coprecipitated into  
403 aragonite in a manner akin to synthetic aragonite formation (FigFig. 2). If this was indeed so this would  
404 nevertheless not contradict our conclusion (see above), namely minorforeign element partitioning into  
405 otoliths involves processes other than aragonite precipitation from an aqueous solution of inorganic ions.  
406 The latter conclusion rests on the behaviour of the other elements as discussed above and is not invalidated  
407 by a putatively different behaviour of Mg and Na. However, the behaviour of Mg and Na might as well  
408 merely appear inorganic numerically (in terms of  $D_e$ ) but the processes underlying  $D_e$  might involve organic  
409 material, i.e. the overall process of partitioning might be very different from inorganic precipitation. This  
410 phenomenon has been described for different calcifiers and is known by the term “invisible vital effect”  
411 (Nehrke & Langer, 2023 and references therein).

412 The likelihood of an invisible vital effect in  $D_e$  is nevertheless much smaller than in the  $D$  calculated  
413 traditionally, i.e. using the external water Me/Ca (seawater or freshwater) as denominator. We added the  
414 traditional partitioning coefficient ( $D_w$ ) to our dataset (FigFig. 2). For Mg and Zn,  $D_w$  falls within the range  
415 of inorganic values, but from this we cannot conclude that Mg and Zn partitioning proceeds via inorganic  
416 precipitation from external water. We know that for ions to enter the endolymph they need to be transported  
417 via the blood (Hüssy et al., 2021; McCormick & Ac Kinlay, 2000; Sturrock et al., 2015) so that there are at  
418 least two partitioning steps operative before the endolymph-otolith step. We look at these partitioning steps  
419 in the following section.

#### 420 4.4 The pathway of minorforeign elements from water to otolith

421 In the freshwater species Sp2 (Fig. 3) and Sp3 (FigFig. Supp-S 2) were the only dataset that allows us to  
422 trace the pathway of minorforeign elements from external water into the otolith. In FigFig. 3 we use Me/Ca  
423 (R) in different reservoirs along the ion transport pathway as given in the literature, and we additionally  
424 calculate two further values: 1) the  $R_{otolith2}$  that results from multiplying  $R_w$  by  $D_{In}$ ; 2) the  $R_{otolith1}$  that results  
425 from multiplying  $R_e$  by  $D_{In}$ . The  $D_{In}$  that are used are selected to minimize the offset between otolith  
426 (measured) and otolith (calculated). The aim of the figures is to illustrate the resulting (R) of different

427 partitioning steps as they actually occur (coloured reservoirs), as opposed to the ones that would  
428 theoretically occur if  $D_{in}$  were applied.

429 Several things can be gleaned from this figure. The first concerns the match / mismatch of otolith and  
430 otolith1. A match indicates that partitioning from endolymph to otolith could be inorganic. This is the case  
431 for Sr, Mg, and Na. Note that the same conclusion can be drawn from Fig. 2 with the exception of  $D_{Sr}$ , which  
432 does not fall within the inorganic range but is close to it. The reason for this discrepancy is that in Fig.  
433 2 a mean and standard deviation is given whereas in Fig. 3 the minimum value of  $D_{in}$  is used. The latter  
434 choice represents a conservative approach aiming at a match between otolith and otolith1. The case of Sr  
435 is therefore borderline, but its behaviour could still be considered inorganic. In stark contrast, the behaviour  
436 of Ba and Zn is clearly not inorganic.

437 ~~The traditional way of calculating partitioning coefficients is from the ambient water to the biomineral. The~~  
438 ~~traditional way of calculating partitioning coefficients is from the water media where the organism lives to~~  
439 ~~the biomineral~~ because the composition of the calcifying fluid is unknown (e.g. Langer et al., 2006). This  
440 poses the central problem of the vital effect. The main question we are asking here is: can the problem of  
441 the vital effect be solved by knowledge of the composition of the calcifying fluid. The answer is yes for Sr  
442 and Na, and no for Ba, Zn, and Mg. Note that  $D_w$  of Zn and Mg show an invisible vital effect, so that using  
443 the correct parent solution can confer no numerical advantage. There is nevertheless knowledge to be  
444 gained. Knowing the values of otolith2 (Zn and Mg) merely tells us that there will be partitioning steps  
445 along the way from water into otolith, but the localization of partitioning along this pathway remains the  
446 classic "black box" (Nehrke & Langer, 2023). Here we can take a look into the black box in unprecedented  
447 detail. The step from water into blood fractionates weakly for Mg but strongly for Zn, while the following  
448 step into the endolymph fractionates weakly against both Mg and Zn. The last step from endolymph to  
449 otolith fractionates strongly against both Zn and Mg. While this step could be inorganic for Mg, it is more  
450 complex for Zn, i.e. the interaction of Zn with organics (as discussed above) contributes to this partitioning  
451 step. Biological partitioning steps are hard to predict in general, and in particular if the ~~minor~~foreign  
452 element and Ca are transported by separate transport systems.

#### 453 4.5 Essential versus non-essential elements

454 While Ca, Na, Mg, and Zn are essential elements, i.e. needed in physiological processes, there is no known  
455 physiological role for Sr and Ba, which are therefore considered non-essential (Lall & Kaushik, 2021;

456 Marshall, 2002; Nielsen, 2004; Salisbury & Ross, 1992). When considering [minor/foreign](#) element  
457 partitioning into biominerals the distinction between essential and non-essential elements is of great  
458 importance because essential elements have their own transport systems while non-essential elements are  
459 thought to pass through the transport systems of essential elements (Langer et al., 2006, 2009). This means  
460 that partitioning from one reservoir into another (e.g. from water into blood) can be conceptualized easier  
461 for non-essential elements, because only the partitioning of individual transport systems has to be known.  
462 If one transport system transports the [minor/foreign](#) element and another transports Ca the situation is more  
463 complicated because the two systems can be regulated independently. In the case of the non-essential  
464 elements Sr and Ba it is usually expected that they partition similarly if not with identical partitioning  
465 coefficient (Allen & Sanders, 1994; Langer et al., 2006, 2009; Nachshen & Blaustein, 1982). It is therefore  
466 surprising that the step from water to blood fractionates for Ba but against Sr, whereas the step from blood  
467 to endolymph does not fractionate at all (or only minimally) for both elements ([Fig. 3](#)). The partitioning  
468 from endolymph to otolith is against both Sr and Ba, i.e. according to expectation. The fact that Ba  
469 fractionation is harder than Sr fractionation could be explained by differential Sr and Ba partitioning of  
470 cellular transporters as well as organic polymers (e.g. Nachshen & Blaustein, 1982; Yuryev et al., 1979).

#### 471 [4.5](#) Conclusion

472 In this study we used literature data on [minor/foreign](#) element composition of the endolymph–otolith system  
473 to calculate partitioning coefficient and analyse the partitioning behaviour of six elements in four species  
474 of fish. The endolymph–otolith system is outstanding because the parent solution (endolymph) of  
475 biomineral (otolith) formation can be sampled, and its elemental composition be determined. Our approach  
476 is novel since up to now the focus on traditional geochemical proxy archives (foraminifers, molluscs, and  
477 coccolithophores) has precluded such an analysis. Our data suggests that:

- 478 1) Otolith mineralization in the endolymph shows a vital effect. Partitioning from endolymph into  
479 otolith is influenced by organic material present in both endolymph and otolith and therefore cannot  
480 be reduced to aragonite precipitation from an aqueous solution of inorganic ions.
- 481 2) Differential partitioning patterns are more complex than generally assumed, as illustrated by the easy-  
482 to-conceptualize “model elements” Sr and Ba, which behave counter to expectation.
- 483 3) Future research should be specifically designed to address elemental partitioning within the  
484 endolymph, as clearly warranted by the findings of this study.

485 Data Availability

486 The data will be published in the “Mendeley data” platform with the reference as [Kekelou, Athina \(2026\),](#)  
487 [“Mineralizing Fluid Control on Foreign Elements in Biogenic CaCO<sub>3</sub>: Insights from Otoliths”, Mendeley](#)  
488 [Data, V3, doi: 10.17632/8ysgz5nb82.3](#) ; [Kekelou, Athina \(2025\), “Trace element incorporation in the fish](#)  
489 [otolith, inorganic crystals vs otoliths”, Mendeley Data, V2, doi: 10.17632/8ysgz5nb82.2](#) . But also they  
490 have been submitted as Supplementary material.

491 Acknowledgments & Declarations

492 **AK** acknowledges funding from the Spanish Ministry of Science and Innovation through the FPI fellowship  
493 (PRE2022-102298) **GL** acknowledges funding from the Spanish Ministry of Universities through a Maria  
494 Zambrano grant and the Generalitat de Catalunya (MERS, 2021 SGR 00640). This work contributes to  
495 ICTA-UAB “María de Maeztu” Programmes for Units of Excellence of the Spanish Ministry of Science  
496 and Innovation (CEX2019-000940-M; [MICIU/AEI/10.13039/501100011033](#)), and the BIOCAL Project  
497 (PID2020-113526RB-I00), and the AEI-DFG project BONITOS ([PCI2025-163190; 541693727](#)).

498 The authors declare that they have no conflict of interest.

499 Author contribution

500 **AK**: Investigation, Formal analysis, Methodology, Data Curation, Writing - Original Draft, Visualization.  
501 **GL**: Conceptualization, Investigation, Writing - Original Draft and Review & Editing, Validation,  
502 Visualization, Project administration **PZ**: Supervision, Visualization, Writing - Review & Editing.

503 Supplementary Material

504 *Supplementary Figures: [Figures-Fig\\_Supp-S1](#) and [Figure-Fig\\_Supp-S2](#) are provided in the separate*  
505 *[supplement file are provided in the appendix. \[FigFig.ure Supp-S1\]\(#\) illustrates the partitioning coefficient \(D\)](#)*  
506 *for Li, comparing the range of the inorganic system and the marine fish (*Acanthopagrus butcheri* - [Sp1](#)).*  
507 *And [Figure-Fig\\_Supp-S2](#) illustrates the Ion transport pathway of the elements Mg, Ba, Na, Sr and Zn in the*  
508 **Salvelinus namaycush* ([Sp3](#)).*

509 Data Excel file: inorganic vs otolith-endolymph

510 Reference

- 511 Albertsen C. M., Hüsey K., Serre S. H., Hemmer-Hansen J., & Thomsen T. B. (2021). Estimating migration  
512 patterns of fish from otolith chemical composition time series. *Canadian Journal of Fisheries and*  
513 *Aquatic Sciences*, 78(10), 1512–1523. <https://doi.org/10.1139/cjfas-2020-0356>
- 514 Allemand D., Mayer-Gostan N., De Pontual H., Boeuf G., & Payan, P. (2007). Fish Otolith Calcification in  
515 Relation to Endolymph Chemistry. *In Handbook of Biomineralization* (pp.291–308).  
516 <https://doi.org/10.1002/9783527619443.ch17>
- 517 Allen G. J., & Sanders D. (1994). Two Voltage-Gated, Calcium Release Channels Coreside in the Vacuolar  
518 Membrane of Broad Bean Guard Cells. *The Plant Cell*, 685–694. <https://doi.org/10.1105/tpc.6.5.685>
- 519 Allen K. A., Hönisch B., Eggins S. M., Haynes L. L., Rosenthal Y., & Yu J. (2016). Trace element proxies  
520 for surface ocean conditions: A synthesis of culture calibrations with planktic foraminifera.  
521 *Geochimica et Cosmochimica Acta*, 193, 197–221. <https://doi.org/10.1016/j.gca.2016.08.015>
- 522 Angell R. W. (1967). The Process of Chamber Formation in the Foraminifer *Rosalina floridana* (Cushman).  
523 *The Journal of Protozoology*, 14(4), 566–574. <https://doi.org/10.1111/j.1550-7408.1967.tb02043.x>
- 524 Avigliano E., Callicó-Fortunato R., Buitrago J., & Volpedo A. V. (2015). A microquímica do otólito é um  
525 indicador do habitat de Mugil curema no sudeste do Mar Caribenho? *Brazilian Journal of Biology*,  
526 75(4), S45–S51. <https://doi.org/10.1590/1519-6984.01014>
- 527 Bareille G., Vignon M., Chappaz A., Fontaine A., Tabouret H., Morat F., Martin J., Aymes J. C., Daverat F.,  
528 Pécheyran C., & Donard O. (2024). Freshwater fish otoliths record signals from both water and  
529 physiological processes: new insights from Sr/Ca and Ba/Ca ratios. *Canadian Journal of Fisheries*  
530 *and Aquatic Sciences*, 81(2), 223–240. <https://doi.org/10.1139/cjfas-2022-0030>
- 531 Bath Martin G., & Thorrold S. (2005). Temperature and salinity effects on magnesium, manganese, and  
532 barium incorporation in otoliths of larval and early juvenile spot *Leiostomus xanthurus*. *Marine*  
533 *Ecology Progress Series*, 293, 223–232. <https://doi.org/10.3354/meps293223>
- 534 Bentov S., & Erez J. (2006). Impact of biomineralization processes on the Mg content of foraminiferal  
535 shells: A biological perspective. *Geochemistry, Geophysics, Geosystems*, 7(1).  
536 <https://doi.org/10.1029/2005GC001015>

537 Bernd R. Schöne, Zengjie Zhang, Dorit Jacob, David P. Gillikin, Thomas Tütken, D.Garbe-Schönberg, Ted  
538 MccoN.Naugey, & Analia Soldati. (2010). Effect of organic matrices on the determination of the trace  
539 element chemistry (Mg, Sr, Mg/Ca, Sr/Ca) of aragonitic bivalve shells (*Arctica islandica*)—  
540 Comparison of ICP-OES and LA-ICP-MS data. *Geochemical Journal*, 44(1), 23–37.  
541 <https://doi.org/10.2343/geochemj.1.0045>

542 BorelliG., Mayer-Gostan N., De Pontual H., Boeuf G., & Payan P. (2001). Biochemical Relationships  
543 Between Endolymph and Otolith Matrix in the Trout (*Oncorhynchus mykiss*) and Turbot (*Psetta*  
544 *maxima*). *Calcified Tissue International*, 69(6), 356–364. [https://doi.org/10.1007/s00223-001-2016-](https://doi.org/10.1007/s00223-001-2016-8)  
545 8

546 Branson O., Redfern S. A. T., Tyliczszak T., Sadekov A., Langer G., Kimoto K., & Elderfield H. (2013).  
547 The coordination of Mg in foraminiferal calcite. *Earth and Planetary Science Letters*, 383, 134–141.  
548 <https://doi.org/10.1016/j.epsl.2013.09.037>

549 Brazier J.-M., Blanchard M., Méheut M., Schmitt A.-D., Schott J., & Mavromatis V. (2023). Experimental  
550 and theoretical investigations of stable Sr isotope fractionation during its incorporation in  
551 aragonite. *Geochimica et Cosmochimica Acta*, 358, 134–147.  
552 <https://doi.org/10.1016/j.gca.2023.08.013>

553 Brazier J. M., Goetschl K. E., Dietzel M., & Mavromatis V. (2024a). Effect of mineral growth rate on Zinc  
554 incorporation into calcite and aragonite. *Chemical Geology*, 643.  
555 <https://doi.org/10.1016/j.chemgeo.2023.121821>

556 Brazier J. M., Harrison A. L., Rollion-Bard C., & Mavromatis V. (2024b). Controls of temperature and  
557 mineral growth rate on lithium and sodium incorporation in abiotic aragonite. *Chemical Geology*,  
558 654. <https://doi.org/10.1016/j.chemgeo.2024.122057>

559 Broecker W. S., & Peng T.-H. (1982). TRACERS IN THE SEA.

560 Bruland K. W. (1989). Complexation of zinc by natural organic ligands in the central North Pacific.  
561 *Limnology and Oceanography*, 34(2), 269–285. <https://doi.org/10.4319/lo.1989.34.2.0269>

562 Campana S. (1999). Chemistry and composition of fish otoliths: pathways, mechanisms and applications.  
563 *Marine Ecology Progress Series*, 188, 263–297. <https://doi.org/10.3354/meps188263>

564 Campana S. E., & Thorrold S. R. (2001). Otoliths, increments, and elements: keys to a comprehensive  
565 understanding of fish populations? *Canadian Journal of Fisheries and Aquatic Sciences*, 58(1), 30–  
566 38. <https://doi.org/10.1139/f00-177>

567 Cavole L. M., Limburg K. E., Gallo N. D., Vea Salvanes A. G., Ramirez-Valdez A., Levin L. A., Oropeza  
568 O. A., Hertwig A., Liu M. C., & McKeegan K. D. (2023). Otoliths of marine fishes record evidence  
569 of low oxygen, temperature and pH conditions of deep Oxygen Minimum Zones. *Deep-Sea Research*  
570 *Part I: Oceanographic Research Papers*, 191. <https://doi.org/10.1016/j.dsr.2022.103941>

571 Checa A. G. (2018). Physical and Biological Determinants of the Fabrication of Molluscan Shell  
572 Microstructures. *Frontiers in Marine Science*, 5. <https://doi.org/10.3389/fmars.2018.00353>

573 Chung M.-T., Trueman C. N., Godiksen J. A., & Grønkjær P. (2019). Otolith  $\delta^{13}\text{C}$  values as a metabolic  
574 proxy: approaches and mechanical underpinnings. *Marine and Freshwater Research*, 70(12), 1747.  
575 <https://doi.org/10.1071/MF18317>

576 Cohen A. L., Gaetani G. A., Lundalv T., Corliss B. H., & George R. Y. (2006). Compositional variability in  
577 a cold-water scleractinian, *Lophelia pertusa*: New insights into “vital effects.” *Geochemistry,*  
578 *Geophysics, Geosystems*, 7(12). <https://doi.org/10.1029/2006GC001354>

579 Crenshaw M. A. (1972). The inorganic composition of molluscan extrapallial fluid. *The Biological Bulletin*,  
580 143(3), 506–512. <https://doi.org/10.2307/1540180>

581 Cuif J.-P., Dauphin Y., & Sorauf J. E. (2010). *Biominerals and Fossils Through Time*. Cambridge University  
582 Press. <https://doi.org/10.1017/CBO9780511781070>

583 Devereux I. (1967). Temperature Measurements from Oxygen Isotope Ratios of Fish Otoliths. *Science*,  
584 155(3770), 1684–1685. <https://doi.org/10.1126/science.155.3770.1684>

585 Dietzel M., Gussone N., & Eisenhauer A. (2004). Co-precipitation of  $\text{Sr}^{2+}$  and  $\text{Ba}^{2+}$  with aragonite by  
586 membrane diffusion of  $\text{CO}_2$  between 10 and 50 °C. *Chemical Geology*, 203(1–2), 139–151.  
587 <https://doi.org/10.1016/j.chemgeo.2003.09.008>

588 D’Olivo J. P., & McCulloch M. T. (2017). Response of coral calcification and calcifying fluid composition  
589 to thermally induced bleaching stress. *Scientific Reports*, 7(1), 2207. [https://doi.org/10.1038/s41598-](https://doi.org/10.1038/s41598-017-02306-x)  
590 [017-02306-x](https://doi.org/10.1038/s41598-017-02306-x)

591 [Druffel E.R.M. \(1997\). Geochemistry of corals: Proxies of past ocean chemistry, ocean circulation,](#)  
592 [and climate. Proc. Natl. Acad. Sci. U.S.A. 94 \(16\) 8354-8361,](#)  
593 <https://doi.org/10.1073/pnas.94.16.8354>

594 Edeyer A., De Pontual H., Payan P., Troadec H., Sévère A., & Mayer-Gostan N. (2000). Daily variations of  
595 the saccular endolymph and plasma compositions in the turbot *Psetta maxima*: relationship with the  
596 diurnal rhythm in otolith formation. In Source: *Marine Ecology Progress Series* (Vol. 192:287-294).

597 Elder K. L., Jones G. A. & Bolz G. (1996). Distribution of otoliths in surficial sediments of the U.S. Atlantic  
598 continental shelf and slope and potential for reconstructing Holocene fish stocks. *Paleoceanography*,  
599 11(3), 359–367. <https://doi.org/10.1029/96PA00042>

600 Elderfield H., Bertram C. J. & Erez J. (1996). A biomineralization model for the incorporation of trace  
601 elements into foraminiferal calcium carbonate. *Earth and Planetary Science Letters*, 142(3–4), 409–  
602 423. [https://doi.org/10.1016/0012-821X\(96\)00105-7](https://doi.org/10.1016/0012-821X(96)00105-7)

603 Elderfield H., & Ganssen G. (2000). Past temperature and  $\delta^{18}\text{O}$  of surface ocean waters inferred from  
604 foraminiferal Mg/Ca ratios. *Nature*, 405(6785), 442–445. <https://doi.org/10.1038/35013033>

605 Fraile I., Arrizabalaga H., Santiago J., Goñi N., Arregi I., Madinabeitia S., Wells R. J. D., & Rooker J. R.  
606 (2016). Otolith chemistry as an indicator of movements of albacore (*Thunnus alalunga*) in the North  
607 Atlantic Ocean. *Marine and Freshwater Research*, 67(7), 1002. <https://doi.org/10.1071/MF15097>

608 Füger A., Konrad F., Leis A., Dietzel M., & Mavromatis V. (2019). Effect of growth rate and pH on lithium  
609 incorporation in calcite. *Geochimica et Cosmochimica Acta*, 248, 14–24.  
610 <https://doi.org/10.1016/j.gca.2018.12.040>

611 Gaetani G. A., & Cohen A. L. (2006). Element partitioning during precipitation of aragonite from seawater:  
612 A framework for understanding paleo proxies. *Geochimica et Cosmochimica Acta*, 70(18), 4617–  
613 4634. <https://doi.org/10.1016/j.gca.2006.07.008>

614 Goetschl K. E., Purgstaller B., Dietzel M., & Mavromatis V. (2019). Effect of sulfate on magnesium  
615 incorporation in low-magnesium calcite. *Geochimica et Cosmochimica Acta*, 265, 505–519.  
616 <https://doi.org/10.1016/j.gca.2019.07.024>

617 Halden N. M., & Friedrich L. A. (2008). Trace-element distributions in fish otoliths: natural markers of life  
618 histories, environmental conditions and exposure to tailings effluence. *Mineralogical Magazine*,  
619 72(2), 593–605. <https://doi.org/10.1180/minmag.2008.072.2.593>

620 Hermann T. W., Stewart D. J., Limburg K. E., & Castello L. (2016). Unravelling the life history of  
621 Amazonian fishes through otolith microchemistry. *Royal Society Open Science*, 3(6), 160206.  
622 <https://doi.org/10.1098/rsos.160206>

623 Hohn S., & Merico A. (2015). Quantifying the relative importance of transcellular and paracellular ion  
624 transports to coral polyp calcification. *Frontiers in Earth Science*, 2.  
625 <https://doi.org/10.3389/feart.2014.00037>

626 Höpker S. N., Wu, H. C., Lucassen F., Sadio O., Brochier T., Nuworkpor I. Y., Kasemann S. A., Merschel  
627 P., & Westphal H. (2022). Sr Isotope Ratios ( $^{87}\text{Sr}/^{86}\text{Sr}$ ) in Water and Fish Otoliths as Estuarine Salinity  
628 Tracers: Case Studies from Three NW African Rivers. *Estuaries and Coasts*, 45(6), 1780–1802.  
629 <https://doi.org/10.1007/s12237-021-01041-x>

630 Hüsey K., Limburg K. E., de Pontual H., Thomas O. R. B., Cook P. K., Heimbrand Y., Blass M., & Sturrock  
631 A. M. (2021). Trace Element Patterns in Otoliths: The Role of Biomineralization. *Reviews in*  
632 *Fisheries Science and Aquaculture* (Vol. 29, Issue 4, pp. 445–477). Taylor and Francis Ltd.  
633 <https://doi.org/10.1080/23308249.2020.1760204>

634 Izzo C., Doubleday Z. A., & Gillanders B. M. (2016). Where do elements bind within the otoliths of fish?  
635 *Marine and Freshwater Research*, 67(7), 1072. <https://doi.org/10.1071/MF15064>

636 Izzo C., Reis-Santos P., & Gillanders B. M. (2018). Otolith chemistry does not just reflect environmental  
637 conditions: A meta-analytic evaluation. *Fish and Fisheries*, 19(3), 441–454.  
638 <https://doi.org/10.1111/faf.12264>

639 Kadan Y., Tollervey F., Varsano N., Mahamid J., & Gal A. (2021). Intracellular nanoscale architecture as a  
640 master regulator of calcium carbonate crystallization in marine microalgae. *Proceedings of the*  
641 *National Academy of Sciences*, 118(46). <https://doi.org/10.1073/pnas.2025670118>

642 Kalish J. M. (1989). Otolith microchemistry: validation of the effects of physiology, age and environment  
643 on otolith composition. *Journal of Experimental Marine Biology and Ecology*, 132(3), 151–178.  
644 [https://doi.org/10.1016/0022-0981\(89\)90126-3](https://doi.org/10.1016/0022-0981(89)90126-3)

645 Kalish J. M. (1991). Determinants of otolith chemistry: seasonal variation in the composition of blood  
646 plasma, endolymph and otoliths of bearded rock cod *Pseudophycis barbatus*. *Marine Ecology*  
647 *Progress Series*, 74, 137–159.

648 Katz M. E., Cramer B. S., Franzese A., Honisch B., Miller K. G., Rosenthal Y., & Wright J. D. (2010).  
649 Traditional and emerging geochemical proxies in foraminifera. *The Journal of Foraminiferal*  
650 *Research*, 40(2), 165–192. <https://doi.org/10.2113/gsjfr.40.2.165>

651 Kawabata T., Takeda Y., Hori M., Kandori K., & Yaji T. (2021). Partitioning of sodium into calcium  
652 carbonates synthesized at 10–40 °C: Influence of organic ligands and temperature. *Chemical*  
653 *Geology*, 559. <https://doi.org/10.1016/j.chemgeo.2020.119904>

654 Kennedy B. P., Klaue A., Blum J. D., Folt C. L., & Nislow K. H. (2002). Reconstructing the lives of fish  
655 using Sr isotopes in otoliths. *Canadian Journal of Fisheries and Aquatic Sciences*, 59(6), 925–929.  
656 <https://doi.org/10.1139/f02-070>

657 Kerr L., Secor D., & Kraus R. (2007). Stable isotope ( $\delta^{13}\text{C}$  and  $\delta^{18}\text{O}$ ) and Sr/Ca composition of otoliths  
658 as proxies for environmental salinity experienced by an estuarine fish. *Marine Ecology Progress*  
659 *Series*, 349, 245–253. <https://doi.org/10.3354/meps07064>

660 Krężel A., & Maret W. (2016). The biological inorganic chemistry of zinc ions. *Archives of Biochemistry*  
661 *and Biophysics*, 611, 3–19. <https://doi.org/10.1016/j.abb.2016.04.010>

662 Lall S. P., & Kaushik S. J. (2021). Nutrition and Metabolism of Minerals in Fish. *Animals*, 11(9), 2711.  
663 <https://doi.org/10.3390/ani11092711>

664 Langer G., Gussone N., Nehrke G., Riebesell U., Eisenhauer A., Kuhnert H., Rost B., Trimborn S., &  
665 Thoms S. (2006). Coccolith strontium to calcium ratios in *Emiliana huxleyi*: The dependence on  
666 seawater strontium and calcium concentrations. *Limnology and Oceanography*, 51(1), 310–320.  
667 <https://doi.org/10.4319/lo.2006.51.1.0310>

668 Langer G., Nehrke G., Thoms S., & Stoll H. (2009). Barium partitioning in coccoliths of *Emiliana huxleyi*.  
669 *Geochimica et Cosmochimica Acta*, 73(10), 2899–2906. <https://doi.org/10.1016/j.gca.2009.02.025>

670 Langer G., Sadekov A., Nehrke G., Baggini C., Rodolfo-Metalpa R., Hall-Spencer J. M., Cuoco E., Bijma  
671 J., & Elderfield H. (2018). Relationship between mineralogy and minor element partitioning in

672 limpets from an Ischia CO<sub>2</sub> vent site provides new insights into their biomineralization pathway.  
673 *Geochimica et Cosmochimica Acta*, 236, 218–229. <https://doi.org/10.1016/j.gca.2018.02.044>

674 Langer G., Sadekov A., Thoms S., Keul N., Nehrke G., Mewes A., Greaves M., Misra S., Reichart G.-J.,  
675 de Nooijer L. J., Bijma J., & Elderfield H. (2016). Sr partitioning in the benthic foraminifera  
676 *Ammonia aomoriensis* and *Amphistegina lessonii*. *Chemical Geology*, 440, 306–312.  
677 <https://doi.org/10.1016/j.chemgeo.2016.07.018>

678 Langer G, Taylor A.R, Walker C.E, Meyer E.M, Ben Joseph O, Gal A, Harper G.M, Probert I, Brownlee C,  
679 Wheeler G.L. (2021) Role of silicon in the development of complex crystal shapes in  
680 coccolithophores. *New Phytol.* 2021 Sep;231(5):1845-1857. doi: 10.1111/nph.17230

681 Lewis G. N., & Randall M. (1921). The activity coefficient of strong electrolytes. *Journal of the American*  
682 *Chemical Society*, 43(5), 1112–1154. <https://doi.org/10.1021/ja01438a014>

683 Limburg K. E., & Casini M. (2018). Effect of marine hypoxia on Baltic Sea cod *Gadus morhua*: Evidence  
684 from otolith chemical proxies. *Frontiers in Marine Science*, 5(DEC).  
685 <https://doi.org/10.3389/fmars.2018.00482>

686 Limburg K. E., Olson C., Walther Y., Dale D., Slomp C. P., & Høie H. (2011). Tracking Baltic hypoxia and  
687 cod migration over millennia with natural tags. *Proceedings of the National Academy of Sciences of*  
688 *the United States of America*, 108(22). <https://doi.org/10.1073/pnas.1100684108>

689 Limburg K. E., Walther B. D., Lu Z., Jackman G., Mohan J., Walther Y., Nissling A., Weber P. K., & Schmitt  
690 A. K. (2015). In search of the dead zone: Use of otoliths for tracking fish exposure to hypoxia. *Journal*  
691 *of Marine Systems*, 141, 167–178. <https://doi.org/10.1016/j.jmarsys.2014.02.014>

692 Longmore C., Trueman C. N., Neat F., O’Gorman E. J., Milton J. A., & Mariani S. (2011). Otolith  
693 geochemistry indicates life-long spatial population structuring in a deep-sea fish, *Coryphaenoides*  
694 *rupestris*. *Marine Ecology Progress Series*, 435, 209–224. <https://doi.org/10.3354/meps09197>

695 Lorens R. B., & Bender M. L. (1980). The impact of solution chemistry on *Mytilus edulis* calcite and  
696 aragonite. *Geochimica et Cosmochimica Acta*, 44, 1265–1278.

697 Lueders-Dumont J. (2024). Postcards from prehistoric marine food webs: nitrogen isotopes in fish otoliths  
698 as a paleoecological archive. <https://doi.org/10.1130/abs/2024AM-403326>

699 Lueders-Dumont J. A., Wang X. T., Jensen O. P., Sigman D. M., & Ward B. B. (2018). Nitrogen isotopic  
700 analysis of carbonate-bound organic matter in modern and fossil fish otoliths. *Geochimica et*  
701 *Cosmochimica Acta*, 224, 200–222. <https://doi.org/10.1016/j.gca.2018.01.001>

702 Marriott C. S., Henderson G. M., Crompton R., Staubwasser M., & Shaw S. (2004). Effect of mineralogy,  
703 salinity, and temperature on Li/Ca and Li isotope composition of calcium carbonate. *Chemical*  
704 *Geology*, 212(1–2), 5–15. <https://doi.org/10.1016/j.chemgeo.2004.08.002>

705 Marshall W. S. (2002). Na (+), Cl (-), Ca (2+) and Zn (+2) transport by fish gills: retrospective review and  
706 prospective synthesis. *Journal of Experimental Zoology*, 293(3), 264–283.  
707 <https://doi.org/10.1002/jez.10127>

708 Martino J. C., Doubleday Z. A., Chung M.-T., & Gillanders B. M. (2020). Experimental support towards a  
709 metabolic proxy in fish using otolith carbon isotopes. *Journal of Experimental Biology*, 223(6).  
710 <https://doi.org/10.1242/jeb.217091>

711 Martino J. C., Doubleday Z. A., Fowler A. J., & Gillanders B. M. (2021). Corrigendum to: Identifying  
712 physiological and environmental influences on otolith chemistry in a coastal fishery species. *Marine*  
713 *and Freshwater Research*, 72(6), 922. [https://doi.org/10.1071/MF20196\\_CO](https://doi.org/10.1071/MF20196_CO)

714 Mavromatis V., Brazier J. M., & Goetschl K. E. (2022). Controls of temperature and mineral growth rate  
715 on Mg incorporation in aragonite. *Geochimica et Cosmochimica Acta*, 317, 53–64.  
716 <https://doi.org/10.1016/j.gca.2021.10.015>

717 Mavromatis V., Goetschl K. E., Grengg C., Konrad F., Purgstaller B., & Dietzel M. (2018). Barium  
718 partitioning in calcite and aragonite as a function of growth rate. *Geochimica et Cosmochimica Acta*,  
719 237, 65–78. <https://doi.org/10.1016/j.gca.2018.06.018>

720 Mavromatis V., Immenhauser A., Buhl D., Purgstaller B., Baldermann A., & Dietzel M. (2017). Effect of  
721 organic ligands on Mg partitioning and Mg isotope fractionation during low-temperature precipitation  
722 of calcite in the absence of growth rate effects. *Geochimica et Cosmochimica Acta*, 207, 139–153.  
723 <https://doi.org/10.1016/j.gca.2017.03.020>

724 McCormick S., & Ac Kinlay D. M. (2000). *Ion Regulation In Fish*. 4th Ed. Prentice-Hall, 85–89.

- 725 McFadden A., Wade B., Izzo C., Gillanders B. M., Lenehan C. E., & Pring A. (2016). Quantitative electron  
726 microprobe mapping of otoliths suggests elemental incorporation is affected by organic matrices:  
727 Implications for the interpretation of otolith chemistry. *Marine and Freshwater Research*, 67(7), 889–  
728 898. <https://doi.org/10.1071/MF15074>
- 729 Melancon S., Fryer B. J., Gagnon J. E., & Ludsin S. A. (2008). Mineralogical approaches to the study of  
730 biomineralization in fish otoliths. *Mineralogical Magazine*, 72(2), 627–637.  
731 <https://doi.org/10.1180/minmag.2008.072.2.627>
- 732 Melancon S., Fryer B. J., Ludsin S. A., Gagnon J. E., & Yang Z. (2005). Effects of crystal structure on the  
733 uptake of metals by lake trout (*Salvelinus namaycush*) otoliths. *Canadian Journal of Fisheries and*  
734 *Aquatic Sciences*, 62(11), 2609–2619. <https://doi.org/10.1139/f05-161>
- 735 Melancon S., Fryer B. J., & Markham J. L. (2009). Chemical analysis of endolymph and the growing  
736 otolith: Fractionation of metals in freshwater fish species. *Environmental Toxicology and Chemistry*,  
737 28(6), 1279–1287. <https://doi.org/10.1897/08-358.1>
- 738 Mellars P. A., Wilkinson M. R., & Fieller N. R. J. (1980). Fish Otoliths as Indicators of Seasonality in  
739 Prehistoric Shell Middens: The Evidence from Oronsay (Inner Hebrides). *Proceedings of the*  
740 *Prehistoric Society*, 46(NA), 19–44. <https://doi.org/10.1017/S0079497X00009300>
- 741 Meyer E. M., Langer G., Brownlee C., Wheeler G. L., & Taylor A. R. (2020). Sr in coccoliths of  
742 *Scyphosphaera apsteinii*: Partitioning behavior and role in coccolith morphogenesis. *Geochimica et*  
743 *Cosmochimica Acta*, 285, 41–54. <https://doi.org/10.1016/j.gca.2020.06.023>
- 744 [Mewes, A., Langer, G., de Nooijer, L. J., Bijma, J., & Reichart, G. J. \(2014\). Effect of different seawater](#)  
745 [Mg<sup>2+</sup> concentrations on calcification in two benthic foraminifers. \*Marine Micropaleontology\*, 113,](#)  
746 [56–64. <https://doi.org/10.1016/j.marmicro.2014.09.003>](#)
- 747 [Mewes, A., Langer, G., de Nooijer, L. J., Reichart, G. J., & Bijma, J. \(2015\). \[Title of paper\]. \*Chemical\*](#)  
748 [Geology](#), [Volume], [Page range]. <https://doi.org/10.1016/j.chemgeo.2015.06.026>
- 749 Miller J. A., & Hurst T. P. (2020). Growth Rate, Ration, and Temperature Effects on Otolith Elemental  
750 Incorporation. *Frontiers in Marine Science*, 7. <https://doi.org/10.3389/fmars.2020.00320>

Field Code Changed

751 Miller M. B., Clough A. M., Batson J. N., & Vachet R. W. (2006). Transition metal binding to cod otolith  
752 proteins. *Journal of Experimental Marine Biology and Ecology*, 329(1), 135–143.  
753 <https://doi.org/10.1016/j.jembe.2005.08.016>

754 Mitsuguchi, T., Matsumoto, E. & Uchida, T. Mg/Ca and Sr/Ca ratios of Porites coral skeleton: Evaluation  
755 of the effect of skeletal growth rate. *Coral Reefs* 22, 381–388 (2003). [https://doi.org/10.1007/s00338-](https://doi.org/10.1007/s00338-003-0326-1)  
756 [003-0326-1](https://doi.org/10.1007/s00338-003-0326-1)

757 Mondal S., Chakrabarti R., & Ghosh P. (2022). A multi-proxy ( $\delta^{44}/40\text{Ca}$ , Sr/Ca, and  $\Delta 47$ ) study of fish  
758 otoliths for determination of seawater temperature. *Chemical Geology*, 605, 120950.  
759 <https://doi.org/10.1016/j.chemgeo.2022.120950>

760 Morat F., Blamart D., Bounket B., Argillier C., Carrel G., & Maire A. (2023). Reconstructing the thermal  
761 history of fish juveniles using stable oxygen isotope analysis of otoliths. *Frontiers in Environmental*  
762 *Science*, 11. <https://doi.org/10.3389/fenvs.2023.1213239>

763 Moura G., Vilarinho L., Santos A. C., & Machado J. (2000). Organic compounds in the extrapalial fluid  
764 and haemolymph of *Anodonta cygnea* (L.) with emphasis on the seasonal biomineralization process.  
765 *Comparative Biochemistry and Physiology Part B: Biochemistry and Molecular Biology*, 125(3),  
766 293–306. [https://doi.org/10.1016/S0305-0491\(99\)00192-3](https://doi.org/10.1016/S0305-0491(99)00192-3)

767 Mucci A., Canuel R., & Zhong S. (1989). The solubility of calcite and aragonite in sulfate-free seawater  
768 and the seeded growth kinetics and composition of the precipitates at 25°C. *Chemical Geology*, 74(3–  
769 4), 309–320. [https://doi.org/10.1016/0009-2541\(89\)90040-5](https://doi.org/10.1016/0009-2541(89)90040-5)

770 Nachshen D. A., & Blaustein M. P. (1982). Influx of calcium, strontium, and barium in presynaptic nerve  
771 endings. *The Journal of General Physiology*, 79(6), 1065–1087.  
772 <https://doi.org/10.1085/jgp.79.6.1065>

773 Nehrke G., Keul, N., Langer G., de Nooijer L. J., Bijma J., & Meibom A. (2013). A new model for  
774 biomineralization and trace-element signatures of Foraminifera tests. *Biogeosciences*, 10(10), 6759–  
775 6767. <https://doi.org/10.5194/bg-10-6759-2013>

776 Nehrke G., & Langer G. (2023). Proxy Archives Based on Marine Calcifying Organisms and the Role of  
777 Process-Based Biomineralization Concepts. *Minerals*, 13(4). <https://doi.org/10.3390/min13040561>

778 Nehrke G., Reichart G. J., Van Cappellen P., Meile C., & Bijma J. (2007). Dependence of calcite growth  
779 rate and Sr partitioning on solution stoichiometry: Non-Kossel crystal growth. *Geochimica et*  
780 *Cosmochimica Acta*, 71(9), 2240–2249. <https://doi.org/10.1016/j.gca.2007.02.002>

781 Nelson T. R., & Powers S. P. (2020). Elemental Concentrations of Water and Otoliths as Salinity Proxies in  
782 a Northern Gulf of Mexico Estuary. *Estuaries and Coasts*, 43(4), 843–864.  
783 <https://doi.org/10.1007/s12237-019-00686-z>

784 Nomaki H., LeKieffre C., Escrig S., Meibom A., Yagyu S., Richardson E. A., Matsuzaki T., Murayama M.,  
785 Geslin E., & Bernhard J. M. (2018). Innovative TEM-coupled approaches to study foraminiferal cells.  
786 *Marine Micropaleontology*, 138, 90–104. <https://doi.org/10.1016/j.marmicro.2017.10.002>

787 Olsher Uriel., Izatt R. M., Bradshaw J. S., & Dalley N. Kent. (1991). Coordination chemistry of lithium  
788 ion: a crystal and molecular structure review. *Chemical Reviews*, 91(2), 137–164.  
789 <https://doi.org/10.1021/cr00002a003>

790 Padilla A. J., Brown R. J., & Wooller M. J. (2015). Strontium isotope analyses ( $^{87}\text{Sr}/^{86}\text{Sr}$ ) of otoliths from  
791 anadromous Bering cisco (*Coregonus laurettae*) to determine stock composition. *ICES Journal of*  
792 *Marine Science*, 72(7), 2110–2117. <https://doi.org/10.1093/icesjms/fsv096>

793 Pallacks S., Ziveri P., Schiebel R., Vonhof H., Rae J. W. B., Little E., Garcia-Orellana J., Langer G.,  
794 Grelaud M., & Martrat B. (2023). Anthropogenic acidification of surface waters drives decreased  
795 biogenic calcification in the Mediterranean Sea. *Communications Earth & Environment*, 4(1), 301.  
796 <https://doi.org/10.1038/s43247-023-00947-7>

797 Payan P., Borelli G., Boeuf G., & Mayer-Gostan N. (1998). Relationship between otolith and somatic  
798 growth: consequence of starvation on acid-base balance in plasma and endolymph in the rainbow  
799 trout *Oncorhynchus mykiss*. In *Fish Physiology and Biochemistry* (Vol. 19).

800 Payan P., Borelli G., Priouzeau F., De Pontual H., Bœuf G., & Mayer-Gostan N. (2002). Otolith growth in  
801 trout *Oncorhynchus mykiss*: supply of  $\text{Ca}^{2+}$  and  $\text{Sr}^{2+}$  to the saccular endolymph. *Journal of*  
802 *Experimental Biology*, 205(17), 2687–2695. <https://doi.org/10.1242/jeb.205.17.2687>

803 Payan P., De Pontual H., Bœuf G., & Mayer-Gostan N. (2004). Endolymph chemistry and otolith growth  
804 in fish. *Comptes Rendus - Palevol*, 3(6-7 SPEC.ISS.), 535–547.  
805 <https://doi.org/10.1016/j.crvp.2004.07.013>

806 Payan P., Edeyer A., Pontual N. DE, Borelli G., Boeuf G., Mayer-Gostan N., Lè ne De Pontual H., & Mayer-  
807 Gostan N. (1999). Chemical composition of saccular endolymph and otolith in fish inner ear: lack of  
808 spatial uniformity. *American physiological society*, 277(1), 123-131,  
809 doi:10.1152/ajpregu.1999.277.1.R123

810 Payan P., Kossmann H., Watrin A., Mayer-Gostan N., & Boeuf G. (1997). Ionic Composition of Endolymph  
811 in Teleosts: Origin and Importance of Endolymph Alkalinity. *Journal of Experimental Biology*,  
812 200(13), 1905–1912. <https://doi.org/10.1242/jeb.200.13.1905>

813 Phillis C. C., Ostrach D. J., Ingram B. L., & Weber P. K. (2011). Evaluating otolith Sr/Ca as a tool for  
814 reconstructing estuarine habitat use. *Canadian Journal of Fisheries and Aquatic Sciences*, 68(2), 360–  
815 373. <https://doi.org/10.1139/F10-152>

816 Pors Nielsen, S. (2004). The biological role of strontium. *Bone*, 35(3), 583–588.  
817 <https://doi.org/10.1016/j.bone.2004.04.026>

818 [Raitzsch, M., Dueñas-Bohórquez, A., Reichart, G.-J., de Nooijer, L. J., & Bickert, T. \(2010\). Incorporation](#)  
819 [of Mg and Sr in calcite of cultured benthic foraminifera: Impact of calcium concentration and](#)  
820 [associated calcite saturation state. \*Biogeosciences\*, 7, 869–881.](#)

821 Rao Z. C., Lueders-Dumont J. A., Stringer G. L., Ryu Y., Zhao K., Myneni S. C., Oleynik S., Haug G. H.,  
822 Martinez-Garcia A., & Sigman D. M. (2024). A nitrogen isotopic shift in fish otolith-bound organic  
823 matter during the Late Cretaceous. *Proceedings of the National Academy of Sciences*, 121(32).  
824 <https://doi.org/10.1073/pnas.2322863121>

825 Reis-Santos P., Gillanders B. M., Sturrock A. M., Izzo C., Oxman D. S., Lueders-Dumont J. A., Hüsey K.,  
826 Tanner S. E., Rogers T., Doubleday Z. A., Andrews A. H., Trueman C., Brophy D., Thiem J. D.,  
827 Baumgartner L. J., Willmes M., Chung M. T., Charapata P., Johnson R. C., ... Walther B. D. (2023).  
828 Reading the biomineralized book of life: expanding otolith biogeochemical research and applications  
829 for fisheries and ecosystem-based management. *Reviews in Fish Biology and Fisheries* 33(2), 411–  
830 449. *Springer Science and Business Media Deutschland GmbH*. [https://doi.org/10.1007/s11160-022-](https://doi.org/10.1007/s11160-022-09720-z)  
831 [09720-z](https://doi.org/10.1007/s11160-022-09720-z)

Field Code Changed

832 Rosales I., Robles S., & Quesada S. (2004). Elemental and Oxygen Isotope Composition of Early Jurassic  
833 Belemnites: Salinity vs. Temperature Signals. *Journal of Sedimentary Research*, 74(3), 342–354.  
834 <https://doi.org/10.1306/112603740342>

835 Sackett D. K., Chrisp J. K., & Farmer T. M. (2024). Isotopes and otolith chemistry provide insight into the  
836 biogeochemical history of mercury in southern flounder across a salinity gradient. *Environmental*  
837 *Science: Processes & Impacts*, 26(2), 233–246. <https://doi.org/10.1039/D3EM00482A>

838 Salisbury F. B., & Ross C. W. (1992). *Plant Physiology*. Wadsworth Publishing Company.

839 Saygin S., Polat N., Willmes M., Lewis L. S., Hobbs J. A., Atıcı A. A., & Elp M. (2022). Strontium isotopes  
840 in otoliths reveal a diversity of natal origins for Tarek (*Alburnus tarichi*) in Lake Van, Turkey.  
841 *Fisheries Research*, 255, 106441. <https://doi.org/10.1016/j.fishres.2022.106441>

842 Shiao J. C., Ložys L., Iizuka Y., & Tzeng W. N. (2006). Migratory patterns and contribution of stocking to  
843 the population of European eel in Lithuanian waters as indicated by otolith Sr:Ca ratios. *Journal of*  
844 *Fish Biology*, 69(3), 749–769. <https://doi.org/10.1111/j.1095-8649.2006.01147.x>

845 [Schöne, B. R., Fiebig, J., Pfeiffer, M., Gleiber, M., Hickson, J., Johnson, A. L. A., ... Oschmann, W. \(2010\).  
846 Environmental controls on shell growth rates and  \$\delta^{18}\text{O}\$  and  \$\delta^{13}\text{C}\$  values in modern freshwater  
847 bivalves \(Unionidae\). \*Geochemical Journal\*, 44, 23–37.](#)

848 Sirost C., Grønkvær P., Pedersen J., Panfili J., Zetina-Rejon M., Tripp-Valdez A., Ramos-Miranda J., Flores-  
849 Hernandez D., Sosa-Lopez A., & Darnaude A. (2017). Using otolith organic matter to detect diet  
850 shifts in *Bardiella chrysoura*, during a period of environmental changes. *Marine Ecology Progress*  
851 *Series*, 575, 137–152. <https://doi.org/10.3354/meps12166>

852 Stanley J. K., & Byrne R. H. (1990). Inorganic complexation of Zinc (II) in seawater. *Geochimica et*  
853 *Cosmochimica Acta*, 54(3), 753–760. [https://doi.org/10.1016/0016-7037\(90\)90370-Z](https://doi.org/10.1016/0016-7037(90)90370-Z)

854 Stoll H., Langer G., Shimizu N., & Kanamaru K. (2012). B/Ca in coccoliths and relationship to calcification  
855 vesicle pH and dissolved inorganic carbon concentrations. *Geochimica et Cosmochimica Acta*, 80,  
856 143–157. <https://doi.org/10.1016/j.gca.2011.12.003>

- 857 Sturrock A. M., Hunter E., Milton J. A., Johnson R. C., Waring C. P., & Trueman C. N. (2015). Quantifying  
858 physiological influences on otolith microchemistry. *Methods in Ecology and Evolution*, 6(7), 806–  
859 816. <https://doi.org/10.1111/2041-210X.12381>
- 860 Sturrock A. M., Trueman C. N., Darnaude A. M., & Hunter E. (2012). Can otolith elemental chemistry  
861 retrospectively track migrations in fully marine fishes? *Journal of Fish Biology*, 81(2), 766–795.  
862 <https://doi.org/10.1111/j.1095-8649.2012.03372.x>
- 863 Sturrock A., Trueman C., Milton J., Waring C., Cooper M., & Hunter E. (2014). Physiological influences  
864 can outweigh environmental signals in otolith microchemistry research. *Marine Ecology Progress  
865 Series*, 500, 245–264. <https://doi.org/10.3354/meps10699>
- 866 Takeuchi T., Sarashina I., Iijima M., & Endo K. (2008). In vitro regulation of CaCO<sub>3</sub> crystal polymorphism  
867 by the highly acidic molluscan shell protein Aspein. *FEBS Letters*, 582(5), 591–596.  
868 <https://doi.org/10.1016/j.febslet.2008.01.026>
- 869 Tanner S. E., Reis-Santos P., Vasconcelos R. P., Fonseca V. F., França S., Cabral H. N., & Thorrold S. R.  
870 (2013). Does otolith geochemistry record ambient environmental conditions in a temperate tidal  
871 estuary? *Journal of Experimental Marine Biology and Ecology*, 441, 7–15.  
872 <https://doi.org/10.1016/j.jembe.2013.01.009>
- 873 Thomas O. R. B., Ganio K., Roberts B. R., & Swearer S. E. (2017). Trace element–protein interactions in  
874 endolymph from the inner ear of fish: implications for environmental reconstructions using fish  
875 otolith chemistry. *Metallomics*, 9(3), 239–249. <https://doi.org/10.1039/c6mt00189k>
- 876 Thomas O. R. B., & Swearer S. E. (2019). Otolith Biochemistry—A Review. In *Reviews in Fisheries  
877 Science and Aquaculture* (Vol. 27, Issue 4, pp. 458–489). Taylor and Francis Inc.  
878 <https://doi.org/10.1080/23308249.2019.1627285>
- 879 Thomas O. R. B., Swearer, S. E., Kapp, E. A., Peng, P., Tonkin-Hill, G. Q., Papenfuss, A., Roberts, A.,  
880 Bernard, P., & Roberts, B. R. (2019). The inner ear proteome of fish. *FEBS Journal*, 286(1), 66–81.  
881 <https://doi.org/10.1111/febs.14715>
- 882 Urey H. C., Lowenstam H. A., Epstein S., & McKinney C. R. (1951). Measurement of Paleotemperatures  
883 and Temperatures of the Upper Cretaceous of England, Denmark, and the Southeastern United States.  
884 *Geological Society of America Bulletin*, 62(4), 399–416.

Field Code Changed

885 Vaisvil A., Willmes M., Enriquez E. J., Klein Z. B., & Caldwell C. A. (2023). A needle in a haystack:  
886 strontium isotopes ( $^{87}\text{Sr}/^{86}\text{Sr}$ ) in otoliths identify origin of largemouth bass from a large Southwest  
887 reservoir. *Canadian Journal of Fisheries and Aquatic Sciences*, 80(12), 1857–1868.  
888 <https://doi.org/10.1139/cjfas-2023-0148>

889 Walker J. M., & Langer G. (2021). Coccolith crystals: Pure calcite or organic-mineral composite structures?  
890 *Acta Biomaterialia*, 125, 83–89. <https://doi.org/10.1016/j.actbio.2021.02.025>

891 Walther B. D. (2019). The art of otolith chemistry: interpreting patterns by integrating perspectives. *Marine  
892 and Freshwater Research*, 70(12), 1643. <https://doi.org/10.1071/MF18270>

893 Walther B. D. & Limburg K. E. (2012). The use of otolith chemistry to characterize diadromous migrations.  
894 *Journal of Fish Biology*, 81(2), 796–825. <https://doi.org/10.1111/j.1095-8649.2012.03371.x>

895 Wells B. K., Campana S. E., & Gillanders B. M. (2014). Otolith chemistry to describe movements and life-  
896 history parameters of fishes: Hypotheses, assumptions, limitations and inferences.  
897 <https://www.researchgate.net/publication/231180600>

898 Wilbur K. M., & Watabe N. (1963). Experimental studies on calcification in molluscs and the alga  
899 *coccolithus huxleyi*. *Annals of the New York Academy of Sciences*, 109(1), 82–112.  
900 <https://doi.org/10.1111/j.1749-6632.1963.tb13463.x>

901 Willmes M., Lewis L. S., Davis B. E., Loiselle L., James H. F., Denny C., Baxter R., Conrad J. L., Fangué  
902 N. A., Hung T. C., Armstrong R. A., Williams I. S., Holden P., & Hobbs J. A. (2019). Calibrating  
903 temperature reconstructions from fish otolith oxygen isotope analysis for California's critically  
904 endangered Delta Smelt. *Rapid Communications in Mass Spectrometry*, 33(14), 1207–1220.  
905 <https://doi.org/10.1002/rcm.8464>

906 Wolthers M., Di Tommaso D., Du Z., & de Leeuw N. H. (2013). Variations in calcite growth kinetics with  
907 surface topography: molecular dynamics simulations and process-based growth kinetics modelling.  
908 *CrystEngComm*, 15(27), 5506. <https://doi.org/10.1039/c3ce40249e>

909 Yuryev V. P., Grinberg N. V., Braudo E. E., & Tolstoguzov V. B. (1979). A study of the boundary conditions  
910 for the gel formation of alginates of polyvalent metals. *Starch - Stärke*, 31(4), 121–124.  
911 <https://doi.org/10.1002/star.19790310406>

- 912 Zazzo A., Smith G. R., Patterson W. P., & Dufour E. (2006). Life history reconstruction of modern and  
913 fossil sockeye salmon (*Oncorhynchus nerka*) by oxygen isotopic analysis of otoliths, vertebrae, and  
914 teeth: Implication for paleoenvironmental reconstructions. *Earth and Planetary Science Letters*,  
915 249(3–4), 200–215. <https://doi.org/10.1016/j.epsl.2006.07.003>
- 916 Zhong S., & Mucci A. (1989). Calcite and aragonite precipitation from seawater solutions of various  
917 salinities: Precipitation rates and overgrowth compositions. *Chemical Geology*, 78 (3-4), 283-299.  
918 [https://doi.org/10.1016/0009-2541\(89\)90064-8](https://doi.org/10.1016/0009-2541(89)90064-8)
- 919 Ziveri P., Stoll H., Probert I., Klaas C., Geisen M., Ganssen G., & Young J. (2003). Stable isotope 'vital  
920 effects' in coccolith calcite. *Earth and Planetary Science Letters*, 210(1–2), 137–149.  
921 [https://doi.org/10.1016/S0012-821X\(03\)00101-8](https://doi.org/10.1016/S0012-821X(03)00101-8)
- 922 Ziveri P., Thoms S., Probert I., Geisen M., & Langer G. (2012). A universal carbonate ion effect on stable  
923 oxygen isotope ratios in unicellular planktonic calcifying organisms. *Biogeosciences*, 9(3), 1025–  
924 1032. <https://doi.org/10.5194/bg-9-1025-2012>